CANDIDATURA MARTA GUARDIOLA

Al Premi Duran Farell d'Investigació Tecnològica, destinat a treballs duts a terme per investigadores a Espanya

1. Resum

El càncer de colon és el càncer més prevalent a Espanya i a molts països d'Europa. Cada any es diagnostiquen gairebé dos milions de casos nous al món i, malauradament, la supervivència als 5 anys és de tan sols el 50%. El motiu d'aquestes xifres és que el mètode estàndard pel diagnòstic del càncer de colon, la colonoscòpia, dista molt de ser perfecte. De fet, el 22% dels pòlips no es detecten amb la colonoscòpia i això provoca que el 8% dels càncers de colon provinguin de colonoscòpies negatives, és a dir, pacients que s'havien fet una colonoscòpia en els sis mesos anteriors i no s'havia detectat res.

Per aquest motiu, l'equip de recerca liderat per la Dra. Marta Guardiola, configurat des de 2019 com a spin-off de l'Hospital Clínic de Barcelona, la Universitat Politècnica de Catalunya, la Universitat Pompeu Fabra i ICREA, està treballant des de fa ja 8 anys en el desenvolupament d'un nou dispositiu mèdic per millorar la detecció del càncer de colon.

Aquest dispositiu, batejat MiWEndo, com la spin-off, consisteix en un radar de microones que empra aquesta revolucionaria tecnologia –la visió per microones– per detectar canvis en les propietats dielèctriques dels teixits. La descoberta que la Dra. Guardiola i el seu equip han documentat és que els canvis en les propietats dielèctriques a la mucosa del colon és un biomarcador pel càncer de colon i així ha estat publicat en revistes científiques de primers quartils.

El dispositiu que ha desenvolupat l'equip de la Dra. Guardiola ha estat miniaturitzat, industrialitzat i patentat en 7 països –Espanya, França, Alemanya, Itàlia, Regne Unit, EUA i Japó–. El dispositiu s'ha dissenyat per actuar com un accessori d'un sol ús pels actuals equips de colonoscòpia. També ha estat validat en estudis preclínics realitzats a l'Hospital Clínic de Barcelona, usant mostres ex vivo de colons humans de 15 pacients i 8 models in vivo porcins.

Fruit d'aquestes validacions, l'Agència Espanyola de Medicaments i Productes Sanitaris ha donat l'autorització per iniciar les validacions clíniques amb quinze primers voluntaris, proves clíniques que ja han començat aquest mateix mes de setembre també a l'Hospital Clínic de Barcelona.

D'altra banda, l'equip que lidera la Dra. Guardiola ha aixecat en 3 anys més de 5,7 milions d'euros provinents de fons privats (1,3 milions) però també de fons públics, incloent un ajut EIC Accelerator de 2,8 milions i un ajut EuroStars de 884.000 €. També el projecte ha obtingut nombrosos reconeixements, locals, nacionals i internacionals, destacant entre molts altres:

- Medalla "Juan López de Peñalver" 2022 atorgada per la Real Academia de Ingeniería.
- Premi Dona TIC 2020 d'Empreneduria atorgat per la Generalitat de Catalunya.
- Premi Salvà i Campillo 2022 atorgat pel Col·legi de Telecomunicacions de Catalunya.
- Finalista del premi "The Spinoff Prize" 2020 organitzat per la revista Nature.
- Premi NAM Healthy Longevity QuickFire Challenge 2020 atorgat per la National Association of Medicine i la farmacèutica Johnson & Johnson.

En aquests moments, a part d'estar executant el primer estudi clínic de la tecnologia, l'equip de la Dra. Guardiola acaba d'obrir una ronda de finançament de 10 milions d'euros per tal de conduir una ronda de validacions clíniques, multicèntriques, a diversos hospitals europeus, com l'Hospital Erasmus de Rotterdam, Uniklinik Köln, Centro Hospitalar Lisboa Norte, l'hospital de KU Leuven, entre d'altres.

2. Descripció del treball

Objectius

L'objectiu del projecte consisteix en desenvolupar i validar clínicament la tecnologia de visió per microones com a eina disruptiva pel diagnòstic mèdic. La primera aplicació en què la Dra. Guardiola i el seu equip està treballant és la detecció precoç del càncer de colon. En aquesta aplicació s'ha desenvolupat i validat preclínicament un dispositiu mèdic en forma d'accessori per un colonoscopi convencional capaç d'avisar al metge amb un senyal acústica de la presència d'un pòlip a temps real mentre aquest realitza una colonoscòpia. L'objectiu a curt termini és aconseguir demostrar la seguretat i la funcionalitat del nostre dispositiu mitjançant dos assajos clínics, un que ja ha començat aquest setembre i l'altre que començarà a principis de l'any vinent. Amb aquestes validacions, a mig termini, les autoritats regulatòries atorgaran la marca CE (Classe IIa) que permetrà comercialitzar el dispositiu a Europa a partir de 2024; així com l'autorització FDA de Novo, que permetrà comercialitzar el dispositiu als EUA. Més endavant s'abordarà el mercat japonès.

L'equip de MiWEndo és pioner en el desenvolupament de dispositius mèdics de visió amb microones miniaturitzats i aptes per a ser introduïts dins el cos humà. Fruit de la recerca realitzada fins al moment i el coneixement adquirit, l'equip de MiWEndo liderat per la Dra. Guardiola, està desenvolupant una plataforma tecnològica aplicable en moltes altres aplicacions en altres àmbits com ara la ginecologia, la odontologia i la reumatologia.

Rellevància tècnica, científica, econòmica i social del treball dut a terme

Aquest projecte suposa un gran avenç per l'automatització del diagnòstic del càncer de colon i per aconseguir la detecció precoç perfecta, dos temes de gran rellevància tècnica, científica, econòmica i social, tal i com es detalla a continuació.

Rellevància científica i tècnica

La rellevància científica del projecte es fa palesa amb la gran i creixent recerca en la millora del diagnòstic del càncer colorectal. En els darrers anys, s'han desenvolupat diversos dispositius i tecnologies per millorar la taxa de detecció de pòlips, com ara endoscopis d'alta definició, endoscopis amb múltiples lents amb capacitat de retrovisió, i accessoris per aplanar la mucosa[1]. La cromoendoscòpia, la microscòpia endoscòpica (endocitoscòpia i endomicroscòpia) o les tècniques hiperespectrals[2] són mètodes desenvolupats per augmentar, millorar i estimar les característiques cel·lulars i del teixit de la mucosa que es poden relacionar amb la malignitat. Totes aquestes tècniques es restringeixen a la informació òptica captada per la càmera i requereixen cada cop més professionals altament formats. Com que els resultats d'aquests mètodes depenen molt de l'experiència de l'operador i del factor humà (fatiga, estrès, resiliència, etc.), una eina capaç d'automatitzar la detecció seria clau per a millorar les taxes de detecció de pòlips. La intel·ligència artificial s'utilitza cada cop més per a l'avaluació en temps real d'imatges endoscòpiques[3]. Tanmateix, si la càmera no visualitza una lesió, no pot ser

[1] W. Ngu Sing and C. Rees, "Can technology increase adenoma detection rate?," *Therap. Adv. Gastroenterol.*, vol. 11, pp. 1–18, 2018.

[2] R. Kumashiro *et al.*, "Integrated endoscopic system based on optical imaging and hyperspectral data analysis for colorectal cancer detection," *Anticancer Res.*, vol. 36, no. 8, pp. 3925–3932, 2016.

[3] G. Urban *et al.*, "Deep Learning Localizes and Identifies Polyps in Real Time With 96% Accuracy in Screening Colonoscopy," *Gastroenterology*, vol. 155, no. 4, pp. 1069-1078.e8, 2018.

detectada per l'algorisme. Els estudis indiquen que el 13,4% de la superfície del còlon podria no visualitzar-se durant una colonoscòpia[4].

La visió o imatge per microones permet escanejar tot el perímetre del còlon i automatitzar la detecció. Aquesta tècnica s'ha desenvolupat durant els últims 40 anys com un mètode de diagnòstic mèdic no ionitzant, de baixa potència i no invasiu, i per tant segur per el pacient, i amb un cost relativament baix[5]. Les microones són capaces d'obtenir imatges anatòmiques i funcionals de l'interior del cos humà a partir del contrast en propietats dielèctriques –la permitivitat relativa i la conductivitat–. S'ha demostrat que les propietats dielèctriques són biomarcadors de molts problemes de salut com l'osteoporosi, l'infart cardíac, l'edema pulmonar, etc., sent el càncer de mama i l'ictus cerebral les aplicacions més investigades. Un sistema de visió per microones consisteix en una agrupació de sensors o antenes convenientment multiplexades per a escanejar completament el cos a estudiar amb un senyal electromagnètic a freqüències d'entre 1-10 GHz. El senyal transmès per les antenes transmissores interacciona amb el teixit humà i finalment es recull a les antenes receptores. Mitjançant un algorisme es pot obtenir el perfil 3D de propietats dielèctriques del teixit a estudiar.

El projecte liderat per la Dra. Guardiola aplica per primera vegada una radiació segura i no-ionitzant, com són les microones, al diagnòstic endoscòpic, i així ho testimonia la patent aprovada internacionalment.

Rellevància econòmica

La rellevància econòmica queda demostrada amb el creixent mercat del càncer de colon a nivell mundial. Malauradament, degut a la creixent incidència del càncer colorectal i en conseqüència a les creixents iniciatives per a la detecció precoç, el nombre de colonoscòpies realitzades, així com el nombre de colonoscopis venuts augmentaran els propers anys.

Els principals mercats de colonoscopis són Alemanya, Itàlia, França, Espanya, Regne Unit, Estats Units i Japó. El mercat total de colonoscopis a aquests països és de 977 milions d'euros el 2020 i es preveu que arribi als 1.311 milions d'euros el 2025 amb una TCAC del 7% entre 2020-2025. En aquests mercats es fan 20,7 milions de colonoscòpies cada any.

Rellevància social

Estem al davant d'un projecte amb un gran impacte social i clínic. Com ja s'ha detallat, en l'actualitat el càncer de colon és el càncer més prevalent en molts dels països desenvolupats. En el cas d'Espanya, el càncer colorectal és el càncer més comú entre homes i dones i la segona causa de mort per càncer, amb més de 41.000 casos nous el 2018. El càncer colorectal descriu malalties canceroses del còlon i el recte. La majoria dels casos de càncer colorectal comencen com un sobrecreixement de teixit, conegut com a pòlip, que s'origina a la superfície del còlon o del recte que creix durant un període de diversos anys. Alguns pòlips (coneguts com a adenomes) són precursors del 90% dels casos de càncer. La taxa global de supervivència a cinc anys del càncer colorectal és d'aproximadament el 65%, però baixa fins al 14,3% si es diagnostica en estadis avançats, cosa que és força comú donada l'absència de símptomes notables quan el càncer es troba en una fase localitzada.

---

[4] J. E. East, B. P. Saunders, D. Burling, D. Boone, S. Halligan, and S. A. Taylor, "Surface visualization at CT colonography simulated colonoscopy: effect of varying field of view and retrograde view," *Am. J. Gastroenterol.*, vol. 102, no. 11, pp. 2529–2535, 2007.

[5] N. K. Nikolova, *Introduction to Microwave Imaging*. Cambridge: Cambridge University Press, 2017.

Afortunadament, estudis científics a gran escala han demostrat que el 90% dels casos poden ser curats amb èxit si es diagnostica la malaltia en etapes precoces. Atesa la importància de la detecció precoç del càncer colorectal per a reduir-ne la incidència i la mortalitat, s'utilitzen diferents proves per al cribratge que permeten la detecció de la població de risc (subjectes positius) combinades amb la colonoscòpia, que és l'única tècnica capaç de detectar i eliminar eficaçment les lesions premalignes i malignes.

No obstant, la colonoscòpia, dista molt de ser perfecta. El camp de visió limitat de la càmera -menys de 180º-, la preparació inadequada del còlon i la subjectivitat de l'exploració depenent de l'experiència de l'endoscopista, entre d'altres, donen lloc a una taxa de no detecció de pòlips del 22% i un risc de desenvolupar càncer després d'una colonoscòpia negativa -l'anomenat càncer d'interval- del 8%. Per tant, el dispositiu dissenyat per la Dra. Guardiola i el seu equip pot complementar de forma molt eficient els actuals colonoscops i alertar als metges endoscopistes mitjançant senyals acústics de la presència de pòlips precancerosos en tota la superfície del colon.

Menció expressa de les aportacions cientificotècniques originals dins de l'àmbit de recerca

Les principals aportacions cientificotècniques originals aportades són les següents:

En primer lloc, la descoberta que amb visió per microones es pot diagnosticar el càncer de colon de manera precoç, o en altres paraules, que les propietats dielèctriques dels pòlips són diferents a les propietats dielèctriques del teixit del colon sa.

En segon lloc, la miniaturització d'un sensor capaç de mesurar els canvis en el camp elèctric produïts per la presència de pòlips al colon. Aquest sensor està integrat en un petit capçal que s'acobla al extrem d'un colonoscopi convencional i està format per una agrupació de 16 antenes multiplexades. Té una llargada màxima de 25 mm i un diàmetre de 20 mm.

Les aportacions científiques es poden trobar en 5 publicacions en revistes científiques realitzades per la Dra. Guardiola i el seu equip, múltiples contribucions en congressos nacionals i internacionals, i 2 patents (una aprovada internacionalment i una sol·licitud de patent).

Principals resultats obtinguts

El projecte sorgeix de la investigació doctoral i postdoctoral realitzada per la Dra. Guardiola en el grup de Teoria del Senyal i Comunicacions de la Universitat Politècnica de Catalunya i subseqüentment a la Universitat Pompeu Fabra al grup BCN MedTech. El 2015, la Dra. Guardiola va iniciar la seva pròpia línia de recerca combinant els seus coneixements en imatge de microones amb una aplicació mèdica no resolta, millorar la detecció precoç del càncer colorectal, en col·laboració amb la Dra. Glòria Fernández Esparrach, endoscopista de l'Hospital Clínic de Barcelona i actual Directora Mèdica de MiWEndo Solutions. Entre el 2015 i el 2019, la Dra. Guardiola va treballar en la prova de concepte i en la primera versió de sensor que es va protegir amb una patent internacional[6].

La prova de concepte va consistir en confirmar que hi havia canvis en les propietats dielèctriques dels pòlips i el teixit del colon sa, donat que no existia bibliografia prèvia en aquest àmbit. Per això la Dra. Guardiola va engegar una campanya de mesures de les propietats dielèctriques de 59 mostres de còlon sa acabat d'extirpar, diferents tipus de pòlips i teixits cancerosos de còlon

[6] https://patents.google.com/patent/WO2017125807A1/pt

de mostres humanes ex vivo entre 0,5 i 20 GHz de 23 pacients sotmesos a colonoscòpies a l'Hospital Clínic de Barcelona. Les mesures es van fer amb una sonda dielèctrica de coaxial obert comercial. Les mesures obtingudes, validades mitjançant anàlisi patològic, van demostrar que les propietats dielèctriques es correlacionen amb el grau de malignitat dels pòlips de colon -com més semblants al càncer, majors són la permitivitat relativa i la conductivitat-. Els resultats inicials van mostrar una sensibilitat del 100% i 91% i una especificitat del 61% i 95% per diferenciar adenocarcinomes i pòlips de mucosa sana. Aquest estudi és la primera demostració de la viabilitat d'utilitzar les propietat dielèctriques per proporcionar informació funcional complementària a la colonoscòpia convencional. Els resultats es van publicar en una revista del primer quartil [1].

El següent pas fou fer un primer prototip de dispositiu no miniaturitzat capaç de mesurar aquests canvis de propietats dielèctriques en colons ex vivo. Val a dir que la sonda utilitzada en la prova de concepte no és vàlida per a ser utilitzada en colonoscòpies ja que requereix contacte continu amb el teixit per a obtenir mesures fiables. En una colonoscòpia en general no hi ha contacte entre el dispositiu i la paret del colon i per tant el dispositiu ha de ser capaç de radiar i rebre ones electromagnètiques a les freqüència de microones amb gran sensibilitat. Per això es va dissenyar, construir i validar unes antenes impreses tipus ranura i alimentades per línia de microstrip. Les antenes són compactes, demostren una bona adaptació a la freqüència de 7.5 GHz -on es va mesurar el màxim de contrast en propietats dielèctriques entre els pòlips i el colon sa-, i presenten baix acoblament entre antenes veïnes. Les antenes es van validar amb simulacions computacionals, i amb models de laboratori anomenats fantomes. Els resultats van demostrar una excel·lent precisió en la detecció de pòlips de 10 mm de diàmetre, i es van publicar en una revista científica de primer quartil [2].

Per finançar aquesta fase de prova de concepte dins la Universitat Pompeu Fabra, la Dra. Guardiola va aconseguir ajudes de concurrència competitiva per valor de 270.000 € de la Generalitat de Catalunya (Indústria del Coneixement modalitat Llavor i Producte), Caixaimpulse de la Fundació La Caixa, Desenvolupament Tecnològic en Salut de l'Institut de Salut Carlos III, i va participar en programes d'acceleració de la Fundació Ship2B i IQS Next Tech. En aquest període el projecte de la Dra. Guardiola va obtenir diversos reconeixements com el Premi del Consell Social de la Universitat Pompeu Fabra al Millor Projecte de Transferència de Tecnologia, el Reconeixement al Projecte d'Impacte Social Ship2B, el Reconeixement com a Projecte Exemplar per les Polítiques de Cohesió de la UE i el Premi Brightlands a l'IQS Tech Fest.

El setembre de 2019 la Dra. Guardiola i la Dra. Fernández van cofundar la spinoff MiWEndo Solutions, disposant d'una prova de concepte sòlida i un equip fundador format, al qual s'hi va unir l'emprenedor en sèrie en el sector de les tecnologies mèdiques, el Dr. Ignasi Belda.

El gener de 2020 la Dra. Guardiola va deixar la universitat pera liderar el projecte dins l'empresa. Els reptes futurs eren majúsculs: formar un equip d'enginyers capaç de desenvolupar un dispositiu preparat per a realitzar estudis en pacients i produir resultats a temps real mentre es realitza la colonoscòpia, amb l'objectiu final de posar en mans dels metges una eina fiable per ajudar-los a detectar precoçment tots els càncers colorectals. Això requereix treballar en 4 àmbits en paral·lel: tecnològic, clínic, regulatori i finançament.

Tecnologia

Entre el 2020 i la primera meitat de 2022, la Dra. Guardiola i el seu equip d'enginyers van treballar en el desenvolupament del dispositiu mèdic de colonoscòpia amb microones.

El sistema consisteix en una combinació de components de maquinari i programari. El maquinari està format per: 1) un dispositiu d'adquisició cilíndric en forma d'anell dissenyat per ser acoblat a la punta d'un colonoscopi convencional, 2) una unitat externa que genera, processa i presenta els resultats i 3) un sistema d'interconnexió entre els dos components anteriors.

El dispositiu d'adquisició és un petit capçal de 25 mm de longitud i 20 mm de diàmetre d'un sol ús i biocompatible que es connecta mitjançant connectors miniatura i cables coaxials ultra fins a la unitat externa. El dispositiu d'adquisició conté dues agrupacions de vuit antenes organitzades en dos anells, un que conté les antenes de transmissió i l'altre les antenes de recepció alimentades per línies microstrip. Per assegurar que el dispositiu és segur per el pacient, s'ha recobert d'una encapsulació i una funda biocompatibles que recobreixen tot el capçal i també els cables que circulen al llarg del colonoscopi. La miniaturització d'aquest dispositiu a un cost molt reduït que faci possible que sigui un fungible ha estat un repte tecnològic novedós i de primer nivell. Prova d'això és el dipòsit d'una nova patent europea titulada "Accessory for an endosope" amb data de sol·licitud 20 de juliol de 2022.

La unitat externa s'encarrega d'emetre un senyal acústic quan es detecta un pòlip a prop de la punta de l'endoscopi durant una colonoscòpia. Aquesta unitat recull el senyal de microones rebut pel dispositiu d'adquisició i el processa mitjançant un algoritme que és capaç d'obtenir els canvis en propietats dielèctriques. Si aquest canvi és substancial, indica la presència d'un pòlip i per tant s'emet un senyal acústic. La unitat externa està formada per un analitzador de xarxes vectorials de 2 ports (VNA) que genera i rep els senyals de microones, un microprocessador, i una pantalla i un timbre per presentar els resultats de la detecció al metge.

El sistema d'interconnexió conté un connector de radiofreqüència i un sistema de multiplexació capaç de seleccionar cada combinació d'antenes transmissora i receptora a gran velocitat. El sistema complet funciona a temps real mentre es realitza una colonoscòpia i és capaç de fer 11 escanejos del colon cada segon. El sistema s'ha dissenyat per no produir canvis en la pràctica clínica de la colonoscòpia per afavorir la seva adopció.

Pel que fa al programari, la Dra. Guardiola i el seu equip han desenvolupat un algoritme format per 3 fases capaç d'emetre una senyal acústica a partir del camp electromagnètic mesurat per el sistema descrit anteriorment. Aquest algoritme està format per 3 parts: la cal·libració, l'enfocament i la detecció. La cal·libració consisteix en netejar el senyal electromagnètic de tots els components no desitjats com ara la paret del colon, soroll provocat per moviments, etc., a la fi que només quedi la contribució d'un possible pòlip. L'enfocament consisteix en formar una imatge a partir del senyal calibrat corresponent a un tall cros-seccional del colon; i finalment la detecció consisteix en identificar automàticament els punts on hi pot haver un pòlip en la imatge anterior per a generar una senyal acústica. L'equip de la Dra. Guardiola s'ha trobat grans reptes en el desenvolupament d'aquest algoritme ja que és un cas molt particular i nou dins la bibliografia existent en visió per microones per una sèrie de motius que es detallen a continuació i ha obligat a desenvolupar mètodes propis. Aquests reptes es deriven de que el nostre sistema s'introdueix a dins del cos i per tant les antenes no envolten el cos a estudiar i la seva posició respecte al teixit és desconeguda.

Validació preclínica i clínica

Aquest sistema s'ha validat preclínicament amb 4 mètodes diferents: simulacions computacionals electromagnètiques, models de laboratori o phantoms, mostres ex vivo i models in vivo.

Simulacions computacionals electromagnètiques

Els models computacionals són cada cop més atractius. L'organisme regulatori americà, la FDA, ha inclòs els models computacionals entre les vuit àrees prioritàries on és essencial un compromís en la investigació científica per avançar en la seva missió reguladora. L'equip de la Dra. Guardiola ha desenvolupat models 3D realistes de colons humans extrets de colonografies computeritzades amb rajos X de pacients reals i els ha associat els propietats dielèctriques mesurades en la prova de concepte. El model permet situar diferents tipus de pòlips en qualsevol posició del colon i moure el model del dispositiu d'adquisició a dins del model de colon i obtenir una simulació del camp electromagnètic tal i com ho faria el dispositiu en un cas real. Donat que la potència computacional necessària es molt important, aquestes simulacions es realitzen mitjançant un sistema de cloud computing implementat per l'equip de la Dra. Guardiola especialment per a aquesta aplicació.

Fantomes

Un pas més en la validació preclínica consisteix en el desenvolupament de models físics o simuladors de colon amb les propietats anatòmiques i dielèctriques d'un còlon humà expandit, anomenat fantoma. La Dra. Guardiola i el seu equip han realitzat 9 models diferents de fantomes de colon cada un pensat per a estudiar de forma aïllada una característica dels colons reals, per exemple la presència de plecs on angulacions o bé l'efecte de la paret del colon. Els fantomes s'utilitzen habitualment en el desenvolupament de sistemes de visió de microones però és la primera vegada que es desenvolupen per a l'aplicació del càncer colorectal i per tant, la Dra. Guardiola i el seu equip han hagut de desenvolupar els seus propis mètodes per realitzar-los. Els fantomes de colon es construeixen mitjançant impressió 3D amb diversos materials que serveixen de motlle per el material que emula les propietats dielèctriques del colon. Aquest material és una barreja d'aigua, gelatina i oli. Variant les proporcions d'aquests ingredients es pot aconseguir variar les propietats dielèctriques per tal d'emular el teixit del colon sa i els diferents tipus de pòlips. Els resultats obtinguts amb fantomes s'han publicat en una revista del primer quartil [3].

Mostres ex vivo

La Dra. Guardiola i el seu equip van examinar 15 colons humans ex-vivo acabats d'extirpar amb càncer (n=12) o pòlips (n=3) amb el dispositiu de visió amb microones a l'Hospital Clínic de Barcelona. Es va desenvolupar un sistema de posicionament per tal d'emular una exploració endoscòpica real amb el fragment de colon ex vivo, es van prendre mesures successives del colon amb el dispositiu i es van processar amb l'algoritme. Després de l'experiment, es van mesurar les propietats dielèctriques de les mostres amb una sonda coaxial i finalment les mostres es van sotmetre a una anàlisi patològic. Els resultats mostren que totes les neoplàsies es van detectar amb una sensibilitat del 100% i una especificitat del 87,4%. Fruit d'aquest treball es van publicar 2 articles en revistes científiques, un en l'àmbit de la tecnologia [4] i l'altre en l'àmbit clínic [5].

Models in vivo porcins

El model més realista de colon és el model porcí. La Dra. Guardiola i el seu equip va realitzar colonoscòpies en 4 porcs sans i en 3 porcs modificats genèticament per desenvolupar pòlips a les instal·lacions d'experimentació endoscopica amb animal gran de l'Hospital Clínic de Barcelona i també en les instal·lacions de la Technische Universität München a Alemanya. Les colonoscòpies es van realitzar adaptant a l'extrem de l'endoscopi el dispositiu de visió amb

microones. Als porcs sans es van simular falsos pòlips injectant 10 mL d'una substància per a injecció submucosa. Amb els 4 porcs sans es va demostrar la seguretat i la intercompatibilitat amb la colonoscòpia convencional . Va ser possible explorar el recte i el còlon descendent sense que el dispositiu interferís amb l'òptica i sense ocasionar cap lesió profunda de la paret, que va ser confirmat en l'anàlisi anatomopatològica. L'ús d'electrocauteri i la instil·lació d'aigua no van interferir amb la funcionalitat de les antenes de microones. Els pòlips (tant falsos com reals) van presentar contrast dielèctric respecte de la mucosa sana i es van poder detectar amb un 100% de sensibilitat. Fruit d'aquest treball s'estan preparant dos article científics, un en una revista de caire tecnològic i un altre en una revista clínica.

Validació Clínica

La fase clínica ha començat oficialment el 16 de setembre de 2022. S'ha realitzat la visita d'inici i ha començat el reclutament de pacients. La validació clínica s'ha planificat en 4 fases:

- Estudi clínic Pilot (fase 1). Estudi pilot prospectiu i únic per demostrar la seguretat de la colonoscòpia amb MiWEndo (N = 15). Els objectius de l'estudi són registrar les incidències i esdeveniments adversos atribuïbles a MiWEndo i la viabilitat de realitzar una colonoscòpia completa: taxa d'intubació cecal, temps per arribar al cec i completar el procediment, percepció de dificultat per part de l'endoscopista, satisfacció del pacient.
- Estudi clínic Pivotal (fase 2). Assaig controlat encreuat, aleatoritzat i únic per comparar l'efectivitat de la colonoscòpia estàndard versus la colonoscòpia estàndard assistida per MiWEndo (N = 50). L'objectiu és avaluar la sensibilitat, l'especificitat, el valor predictiu positiu, el valor predictiu negatiu i la precisió de la colonoscòpia assistida per MiWEndo per a la detecció d'adenomes i pòlips, així com els paràmetres de seguretat. S'extreurà les lesions i es realitzarà l'anàlisi patològic, que és l'estàndard d'or per al diagnòstic dels pòlips.
- Fase 3. Desenvolupament de la pràctica (DOP). L'objectiu d'aquesta etapa és familiaritzar la pràctica dels endoscopistes, s'estudiarán N=60 pacients repartits en els hospitals que participen en la fase 4.
- Fase 4. Assaig clínic multicèntric, aleatoritzat, paral·lel i comparatiu per comparar la taxa de detecció d'adenoma (ADR) de la colonoscòpia assistida per MiWEndo amb la colonoscòpia estàndard (n = 898).

Regulatoria

La regulació de dispositius mèdics és una part clau en el desenvolupament de dispositius mèdics. El seu objectiu és oferir productes amb els nivells de qualitat i rendiment necessaris per a un dispositiu mèdic i és necessari per obtenir l'autorització de comercialització. Així, la regulatòria està estretament lligada al procés de disseny, desenvolupament i validació. Tant el disseny com la validació del dispositiu s'han fet seguint les recomanacions especificades en la legislació vigent de dispositius mèdics, MDR o Regulació (EU) 2017/745 i estàndards i normes harmonitzades o ISO.

L'agost de 2022, MiWEndo Solutions va aconseguir l'autorització de l'Agència Espanyola del Medicament per a realitzar l'estudi clínic Pilot que és el primer estudi en humans amb el dispositiu de MiWEndo que ha començat aquest setembre. Actualment s'està treballant amb la presubmissió amb l'entitat regulatòria americana FDA i amb el sistema de qualitat de l'empresa.

Finançament

Pel que fa al finançament l'equip que lidera la Dra. Guardiola ha aixecat en 3 anys més de 5,7 milions d'euros provinents de fons privats (1,3 milions) però també de fons públics, a destacar un ajut de l'EIC Accelerator de 2,8 milions i un ajut EuroStars de 884.000 €.

També el projecte ha obtingut nombrosos reconeixements, locals, nacionals i internacionals, destacant entre molts altres:

- Medalla "Juan López de Peñalver" 2022 atorgada per la Real Academia de Ingeniería.
- Premi Dona TIC 2020 d'Empreneduria atorgat per la Generalitat de Catalunya.
- Premi Salvà i Campillo 2022 atorgat pel Col·legi de Telecomunicacions de Catalunya.
- Finalista del premi "The Spinoff Prize" 2020 organitzat per la revista Nature.
- Premi NAM Healthy Longevity QuickFire Challenge 2020 atorgat per la National Association of Medicine i la farmacèutica Johnson & Johnson.
- Semifinalists of premios Fundación Mafpre a la Inovación Social 2020, Premi Societat Catalana de Biologia Startup 2020,
- Premi National Association of Medicine i la farmacèutica Johnson & Johnson dotat amb 250.000 $ el 2022.

Impacte del treball a curt i llarg termini

L'impacte del grup liderat per la Dra. Guardiola en el curt termini ha estat la creació de 14 llocs de treball altament qualificats, dels quals el 50% són dones i el 50% són doctors o doctores en diverses àrees de la bioenginyeria: telecomunicacions, electrònica, informàtica, medicina, enginyeria biomèdica, biotecnologia, etc. Aquests llocs de treball són altament qualificats ja que 4 són doctors i la resta disposa d'estudis superiors i Master. MiWEndo també aposta per la formació dels seus treballadors, de fet la Dra. Guardiola dirigeix 2 doctorats industrials pel quals s'han obtingut ajudes del ministeri de ciència i innovació.

En canvi, en el llarg termini, més enllà dels llocs de treball planificats que s'han de crear per prosseguir en la fabricació i comercialització del dispositiu a gran escala −més de 30 de llocs addicionals−, l'impacte principal vindrà dels usuaris de la tecnologia i, sobretot, de les vides salvades.

L'impacte socioeconòmic de MiWEndo quantificat amb el mètode SROI és de 9,8: el valor social és gairebé deu vegades més gran que la inversió necessària. MiWEndo reduirà el càncer colorectal d'interval millorant la taxa de detecció de pòlips. A més, contribuirà a la sostenibilitat dels sistemes sanitaris de la UE i mundials reduint el temps d'exploració, la repetició de colonoscòpies i el nombre d'anàlisis patològiques, així com els costos del tractament del càncer colorectal. D'aquesta manera, MiWEndo tindrà un impacte positiu substancial en els pacients i les seves famílies en termes de vides salvades estimades en 87.000/any a Europa i en qualitat de vida.

L'estratègia de sortida al mercat començarà als centres de Catalunya i Espanya l'any 2024 suposant una utilització del 90% de l'accessori de MiWEndo i una taxa de penetració del 0,16% l'any 2024. L'any 2025 haurem incrementat la nostra xarxa de vendes en Espanya i penetrarem als mercats espanyol, francès, alemany i britànic. Com que aquest projecte compta amb la participació de 5 hospitals de referència europeus diferents, al final del projecte ja tindrem contactes existents amb importants KOL i col·laboracions prèvies establertes en alguns dels nostres mercats objectiu. Aquest fet facilitarà la implementació de MiWEndo. El 2026, esperem continuar augmentant la nostra taxa de penetració i començar a vendre el nostre dispositiu a la

resta dels nostres mercats objectiu; Unió Europea, Japó i EUA. Finalment, l'any 2030 esperem que 21.575 centres utilitzin MiWEndo en el 90% de les colonoscòpies, de manera que, basant-nos en aquestes hipòtesis, esperem una taxa de penetració del 38,19% i un total de 5.627.088 unitats venudes.

Pel que fa a l'impacte en la salut, segons les nostres projeccions, 1 milió de persones a tot el món es beneficiaran de la nostra solució en 3 anys després de la finalització del projecte (2027). Les projeccions han considerat el següent mercat de penetració: França (130 k), Alemanya (77 k), Itàlia (92 k), Espanya (29 k), Altres UE (53 k), Regne Unit (27 k), EUA (321 k), Japó (146 k), Altres (128 k). Per tant, només a la UE-27, un total de 407.000 pacients es beneficiaran de la nostra solució, augmentant aquest nombre a 1,5 milions de persones el 2030.

Patents i llicències que s'han derivat del treball

El treball ha aconseguit fins la data dues patents i se està treballant en dues més.

La primera d'elles, una patent europea, ja està aprovada a 7 països −Espanya, França, Itàlia, Japó, Regne Unit, Alemanya i els EUA−, amb codi WO2017125807A1. Aquesta patent és titularitat de la Universitat Pompeu Fabra, la Universitat Politècnica de Catalunya, l'Hospital Clínic de Barcelona i ICREA i té com a autors: Miguel Angel González Ballester, Oscar Camara Rey, Marta Guardiola Garcia, Mario Ceresa, Maria Gloria Fernández Esparrach i Jordi Romeu Robert. La patent fou llicenciada a la spin-off que lidera la Dra. Guardiola en data d'octubre del 2019. Aquesta patent protegeix, de manera molt genèrica, l'ús de les microones per qualsevol tipus de diagnòstic clínic endoscòpic.

La segona de les patents fou dipositada en l'Oficina Espanyola de Patents i Marques en data de prioritat de 29 de juliol del 2022 i codi P5852EP00. La patent, doncs, encara no ha entrat en la fase internacional, però d'acord als estudis de patentabilitat realitzats, no s'espera que les autoritats examinadores interposin cap mena d'impediment. La primera patent protegeix el concepte bàsic de l'ús de les microones pel diagnòstic clínic endoscòpic, mentre que la segona protegeix el dispositiu mèdic concret dissenyat i desenvolupat pel diagnòstic del càncer de colon per via endoscòpica.

Finalment, en aquests moments s'està treballant en una tercera i una quarta patent, que està elaborant el despatx especialitzat ZBM. La idea és depositar al mateix temps ambdues patents per tal de no interferir en l'activitat inventiva de l'una sobre l'altra. El que es vol patentar en aquestes dues noves patents és l'aplicació de les microones a noves àrees diagnòstiques, en concret, en ginecologia −patologies de l'endometri− i reumatologia −artritis i artrosi−. En el futur es treballarà també en altres patents de nous dispositius aplicats a altres àrees.

Procedència dels fons amb què s'ha finançat del treball

El grup de la Dra. Guardiola ha aixecat més de 5,7 milions d'euros al llarg dels anys, tant en la seua etapa acadèmica com en l'empresarial. En l'etapa acadèmica es van obtenir 270.000 € provinents de l'AGAUR −100.000 € Ajuts Producte i 25.000 € Ajuts Llavor−, l'Instituto Carlos III −75.000 € Desarrollo Tecnológico en Salud− i La Caixa −70.000 € CaixaImpulse−.

En l'etapa empresarial el projecte ha aixecat el següent finançament:

- 1.300.000 € de fonts privats, incloent la Fundación Botín −500.000 €−, BStartup −100.000 €, i diversos fons familiars privats catalans.
- 2.800.000 € provinents de la Comissió Europea i el Banc Europeu d'Inversions a través del programa EIC Accelerator.

- 884.000 € provinents del programa europeu EuroStars d'Eureka.
- $250.000 provinents de la National Asociation of Medicine a través del programa Healthy Longevity QuickFire Challenge 2020.
- 71.000 € provinents del Ministeri de Ciència i Innovació a través del programa de doctorats industrials.
- 50.000 € provinents de la institució europea EIT Health a través del programa HeadStart.
- Aproximadament 100.000 € d'altres fonts menors com Ajuntament de Barcelona, AGAUR, Hospital Clínic de Barcelona, Oficina Europea de Patents i Marques, etc.

3. Llista de publicacions relacionades amb el resultat de la recerca i còpia de les tres publicacions més rellevants

1. Marta Guardiola, Santiago Buitrago, Glòria Fernández-Esparrach, Joan M O'Callaghan, Jordi Romeu, Miriam Cuatrecasas, Henry Córdova, Miguel Ángel González Ballester, Oscar Camara. Dielectric properties of colon polyps, cancer, and normal mucosa: Ex vivo measurements from 0.5 to 20 GHz. Medical physics, 8, pp. 3768-3782, 2018.
2. Marta Guardiola, Kahina Djafri, Mouloud Challal, Miguel A González Ballester, Gloria Fernandez-Esparrach, Oscar Camara, Jordi Romeu. Design and evaluation of an antenna applicator for a microwave colonoscopy System. IEEE Transactions on Antennas and Propagation, 67(8), pp. 4968-4977, 2019.
3. Alejandra Garrido, Roberto Sont, Walid Dghoughi, Sergi Marcoval, Jordi Romeu, Glòria Fernández-Esparrach, Ignasi Belda, Marta Guardiola. Automatic polyp detection using microwave endoscopy for colorectal cancer prevention and early detection: Phantom validation. IEEE access, 9, pp. 148048-148059, 2021.
4. Marta Guardiola, Walid Dghoughi, Roberto Sont, Alejandra Garrido, Sergi Marcoval, Luz María Neira, Ignasi Belda, Glòria Fernández-Esparrach. MiWEndo: Evaluation of a Microwave Colonoscopy Algorithm for Early Colorectal Cancer Detection in Ex Vivo Human Colon Models. Sensors, 2022.
5. Glòria Fernández-Esparrach, Alejandra Garrido, Roberto Sont, Walid Dghoughi, Sergi Marcoval, Miriam Cuatrecasas, Sandra López-Prades, F Borja de Lacy, María Pellisé, Ignasi Belda, Marta Guardiola. Microwave-Based Colonoscopy: Preclinical Evaluation in an Ex Vivo Human Colon Model. Gastroenterology Research and Practice, 2022, article ID: 9522737.

IEEE Access
Multidisciplinary | Rapid Review | Open Access Journal

Received September 28, 2021, accepted October 26, 2021. Date of publication xxxx 00, 0000, date of current version xxxx 00, 0000.

Digital Object Identifier 10.1109/ACCESS.2021.3124019

Automatic Polyp Detection Using Microwave Endoscopy for Colorectal Cancer Prevention and Early Detection: Phantom Validation

ALEJANDRA GARRIDO[1], ROBERTO SONT[1], WALID DGHOUGHI[1], SERGI MARCOVAL[1], JORDI ROMEU[2], (Fellow, IEEE), GLÒRIA FERNÁNDEZ-ESPARRACH[1,3], IGNASI BELDA[1], AND MARTA GUARDIOLA[1]

[1]MiWEndo Solutions, 08014 Barcelona, Spain
[2]CommSensLab, Universitat Politècnica de Catalunya (UPC), 08034 Barcelona, Spain
[3]Endoscopy Unit, Department of Gastroenterology, Hospital Clínic, CIBEREHD, IDIBAPS, University of Barcelona, 08036 Barcelona, Spain

Corresponding author: Marta Guardiola (marta@miwendo.com)

The work of Alejandra Garrido was supported by DIN2019-010857. The work of Roberto Sont, Ignasi Belda, and Marta Guardiola was supported in part by the European Union's Horizon 2020 Research and Innovation Programme under Grant 960251 and in part by the European Institute of Innovation and Technology (EIT). The work of Jordi Romeu was supported by PID2019-107885GB-C31/AEI/10.13039/501100011033.

ABSTRACT A system to integrate microwave imaging with optical colonoscopy is presented. The overarching goal is to improve the prevention and early diagnosis of one of the main health and economic burdens of an increasingly aging population, i.e., colorectal cancer. For a colonoscopy, the gold standard for colorectal cancer diagnosis, 22% of polyps are not detected, and the risk of cancer after a negative colonoscopy can be up to 7.9%. To remedy this, a microwave imaging system able to generate an alarm when a polyp is detected is designed, manufactured and validated with a colon phantom composed of tissue-mimicking oil-gelatin materials reproducing the anatomy and dielectric properties of a human colon with a polyp. The acquisition was performed by a miniaturized ring-shaped switched array of 16 antennas attachable at the tip of a conventional colonoscope. This has been conceived to satisfy endoscopy size restrictions, patient safety and intercompatibility with current clinical practice. A Modified Monofocusing imaging method preceded by a previous frame average subtraction as a calibration technique shows a perfect detection of a 10-mm polyp (100% sensitivity and specificity) in the eight analyzed trajectories. The phantom results demonstrate the feasibility of the system in future preclinical trials.

INDEX TERMS Backpropagation algorithms, endoscopes, medical diagnostic imaging, microwave antenna arrays, microwave imaging.

I. INTRODUCTION

Globally, 1.93 million new cases of colorectal cancer (CRC) are diagnosed annually, with 935,000 people dying from CRC in 2020 [1]. This has led to CRC being the second most common cause of cancer death in both men and women. CRC describes cancerous malignancies of the colon and rectum. Most cases of CRC begin as a growth of tissue, known as a polyp, which originates in the lining of the colon or rectum and grows in size over a period of several years. Polyps are common in patients over 50 years, but certain polyps (known as adenomas) are estimated to be precursors to 90% of CRC cases [2]. The overall five-year survival rate of CRC is approximately 65%, but drops to 14.3% if diagnosed at advanced stages, which is quite common given the absence of remarkable symptoms when the cancer is in a localized phase [3].

Large-scale studies have found that CRC can be cured in more than 90% of cases if adenomas are removed[2]. Optical colonoscopy is the most effective method for CRC diagnosis and is the only method that is able to remove polyps in the entire colon. During a colonoscopy, a long, flexible tube called a colonoscope is inserted into the rectum. A tiny video camera at the tip of the tube allows the doctor to view the

The associate editor coordinating the review of this manuscript and approving it for publication was Chulhong Kim.

This work is licensed under a Creative Commons Attribution 4.0 License. For more information, see https://creativecommons.org/licenses/by/4.0/

inside of the entire colon. However, the limited field of view of the camera (less than 180°), inadequate colon preparation and the subjectivity of the exploration dependent on the endoscopist's experience, among others, result in a polyp miss rate of 22% [4] and a risk of developing cancer after a negative colonoscopy, the so-called interval CRC of 8% [5].

In recent years, several devices and technologies have been developed to improve the detection rate of polyps such as high-definition endoscopes, endoscopes with multiple lenses (retrovision capability), and mucosal flattening accessories [6]. Chromoendoscopy, endoscopic microscopy (endocytoscopy and endomicroscopy) or hyperspectral techniques [7] are methods developed to magnify, enhance and estimate mucosal tissue and cell characteristics that can be linked to malignancy. All of these techniques are restricted to the optical information captured by the camera and increasingly require highly trained professionals. Because the outcomes of these methods are highly dependent on the operator's experience and human factors (fatigue, stress, resilience, etc.), a tool capable of automating the detection is needed. Artificial intelligence is increasingly used for the real-time assessment of endoscopic images [8]. However, if a lesion is not visualized by the camera, it cannot be detected by the algorithm. Studies indicate that 13.4% of the colon surface area might not be visualized during a standard colonoscopy [9], [10].

Microwave imaging allows us to scan 360° of the colon and automate detection. It has been developed for the last 40 years as a portable, non-ionizing, low-power, non-invasive, and low-cost medical diagnostic method [11] that is able to obtain anatomical and functional images of the interior of the human body based on the contrast in dielectric properties, i.e., the relative permittivity and the conductivity. Dielectric properties are biomarkers of many health problems, such as osteoporosis [12], heart infarction [13], pulmonary edema, etc., with breast cancer [14], [15] and brain stroke [16], [17] being the most researched and advanced topics. We recently demonstrated that the dielectric properties correlate with the malignancy grade of colon polyps [18]; the more similar to cancer, the higher the relative permittivity and conductivity. The results indicate that the maximum contrast between healthy mucosa and cancer was 30% and 90% for the relative permittivity and conductivity, respectively, at 8 GHz.

Table 1 shows how the proposed microwave endoscopy system compares with the gold standard, i.e., conventional colonoscopy, advanced colonoscopy techniques [6], mucosa flattening accessories [19] and deep learning-assisted colonoscopy [20]. The ADR, or Adenoma Detection Rate, is defined as the percentage of patients undergoing screening colonoscopy who have one or more adenomas detected and is the quality indicator of colonoscopy. ADR is not yet available for microwave endoscopy since it has not been used in humans so far. The ADR increase is measured with respect to a conventional colonoscopy.

This paper reports a system to integrate microwave imaging with optical colonoscopy aimed at improving the prevention and early detection of colorectal cancer. To the best of our knowledge, this is the first time that microwave imaging has been proposed for endoscopic applications. With the proposed system, the detection of polyps can be automatized by generating an alarm when a polyp is detected in order to warn the endoscopist. As the proposed system is an add-on to standard colonoscopy, if the alarm goes off and the polyp is not visualized with colonoscopy, then the doctor can better examine the area to find it. This feature will fill the gap between endoscopists with different levels of experience, which has been demonstrated to play an important role in colonoscopy effectiveness and moves forward a major trend of the automating medical explorations field.

TABLE 1. Performance comparison between different colon visualization methods.

Method	Field of view	Automatic detection	ADR increase
Conventional colonoscopy	<170°	No	-
High definition colonoscopy	<170°	No	4.5%
Magnification colonoscopy	<170°	No	0%
Chromoendoscopy	<170°	No	0%
Multi-lens colonoscopy	235°-360°	No	5%
Deep learning	- [1]	Yes	14%
Flattening accessories	<170°	No	16%
Microwave endoscopy	360°	Yes	N/A

[1] The field of view depends on the colonoscope it is attached to.

The proposed acquisition system has to adapt and be robust to established colonoscopy clinical practice, which entails a series of peculiarities with respect to previous microwave imaging systems reported in the literature [21], [22]. As an advantage, there is no need to penetrate the body since polyps are superficial lesions. However, a number of challenges have emerged. On one hand, space restrictions limit the number of antennas in the array, reduce the size and thickness of each antenna element and increase the mutual coupling between them. Electrically small antennas are narrowband, limiting the range of imaging algorithms to frequency domain algorithms. On the other hand, the antennas are distributed in a circular array enclosed by the imaging region instead of the imaging region being surrounded by the antennas, which is the usual configuration for microwave imaging. Finally, the unknown and changing distance from the imaging region with respect to the antenna array increases the degrees of freedom introduced by the uncertainty of the spatial and temporal delay reception of the scattered fields. Therefore, calibration methods to eliminate all unwanted effects other than the target (the polyp) are essential.

The microwave endoscopy system is verified with a colon phantom that allows to simulate a colonoscopy exploration. The phantom models a section of colon and is composed of gelatin-oil-based materials to mimic the dielectric properties of healthy colon mucosa and polyps. The reconstructed images from the phantom are quantitatively analyzed in terms of efficacy for different calibration methods.

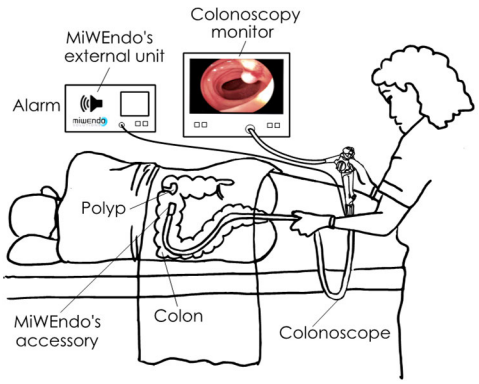

FIGURE 1. MiWEndo's microwave endoscopy system is composed of an accessory attachable at the distal tip of a standard colonoscope and an external processing unit. MiWEndo generates an alarm when a polyp is detected to warn the endoscopist.

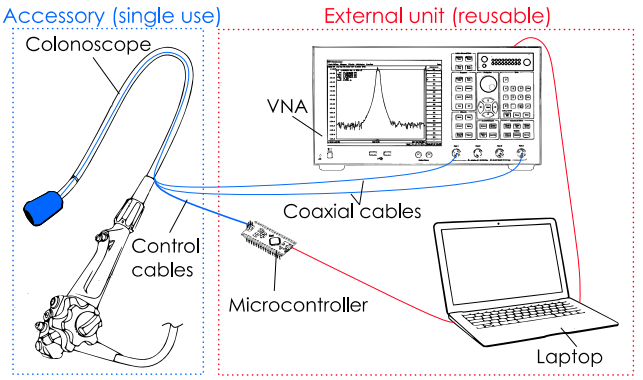

FIGURE 2. The Imaging system consists of a cylindrical ring-shaped acquisition device (in blue in the picture) attached to the end of a colonoscope and connected via cables to the external unit. The external unit consists of a vector network analyzer, a microcontroller, and a laptop.

II. MICROWAVE ENDOSCOPY SYSTEM

The imaging system consists of a combination of hardware and software components. The hardware is composed of: 1) a cylindrical ring-shaped acquisition device designed to be attached to the tip of a conventional colonoscope and 2) an external unit with a microwave transceiver, and controlling and processing units. The acquisition device is connected via cables to the external unit. The acquisition device contains two switched arrays of eight antennas organized in two rings, with one containing the transmitting antenna and the other containing the receiving antenna fed by microstrip lines. The antenna arrays are multiplexed by a two single-pole-eight-throw (SP8T) radiofrequency switches. The external unit is composed by a 2-port vector network analyzer (VNA) Keysight E5071C, a microcontroller Arduino Nano and a laptop. The VNA generates and receives the microwave signals to obtain the S-parameters and is connected to a laptop that controls the measurement. The microcontroller translates the switches' control sequences to two 3 bit codes of 0-5 V signals. Two slim coaxial cables with a diameter of 1.13 mm and a length of 500 mm transmit the microwave signals, and eight copper cables transmit the switches' control signals. Miniature connectors are used for a non-bulky final assembly. Fig. 1 shows how the microwave endoscopy system will work in clinical practice, and Fig. 2 shows the block diagram of the proposed system.

The antenna elements are cavity-backed slot antennas, as described in our previous paper [23], and are shown in Fig. 3(a). The antennas have been assembled onto a polyamide flexible printed circuit board that contains the microstrip feeding lines and the two radiofrequency switches. This assembly is wrapped around a cylindrical metallic 3D printed ring that has 16 cavities on its surface to house the antennas. The colonoscope tip can be inserted into the ring hole. The printed circuit board is covered with an encapsulation made of a biocompatible heat shrink tubing to protect the circuit from moisture and the patient from lesions. The final dimensions of the acquisition device are 30 mm in length by 20 mm in diameter, with a total

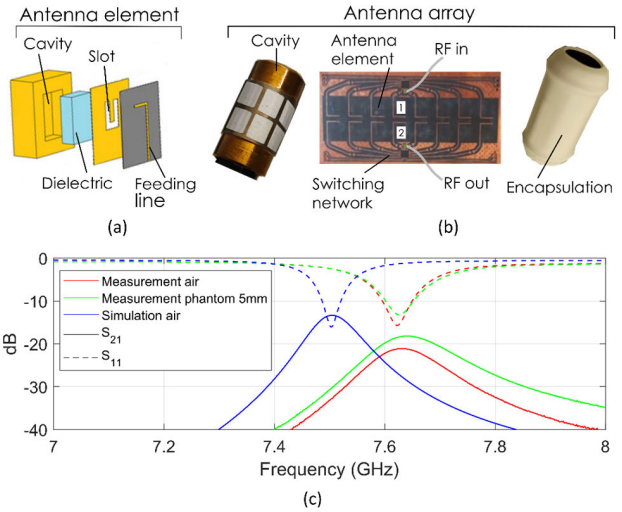

FIGURE 3. Antenna array: (a) The antenna element is a cavity-backed slot antenna; (b) The antenna array is composed by two rings of eight antennas mounted on a flexible substrate, wrapped on a cylindrical metallic cavity and protected by a plastic encapsulation; (c) Comparison between the measured and simulated reflection and the transmission coefficients in air and with a phantom.

thickness of 3 mm. The dimensions and shape of the device ensure non-obstruction of the front tip of the colonoscope, avoids camera concealment, injures the patient, or hinders the maneuverability of the colonoscope.

Fig. 3(c) shows the transmission and reflection coefficients measured and simulated with the central pair of transmitting and receiving antennas in the array (indicated in Fig. 3(b)). We compared the S-parameters in air with a phantom of healthy mucosa tissue situated at 5 mm from the antenna surface. In air, the antennas operate over the band 7.6-7.66 GHz, which is an approximately 0.8% fractional bandwidth with respect to the center frequency of 7.63 GHz, assuming a -10 dB reflection coefficient as a reference. The reason for such a small bandwidth is the miniaturization of the antennas ($0.12\lambda \times 0.16\lambda$). Since the antennas are very close one another, the mutual coupling increases, introducing error into the measured scattered field. Cavity-backed antennas

have been used to minimize coupling to −13 dB. The comparison between the measured and simulated results in free space shows a slight frequency shift and increased losses in the measured results. The main difference between the simulated and the measured results is the higher losses in the measurement, which are clearly seen on both the reflection and transmission S-parameters. These losses are mainly produced by the metallization roughness and welding, which is not considered in the simulation. By comparing the measurements in air with the measurements with the phantom, we can observe that the presence of the phantom affects both the transmission and reflection parameters; in fact, the input impedance matching is improved while the resonant frequency is almost the same. To obtain the measurement results at the antenna plane and remove the effects of the long cables, a Thru, Reflect, Line (TRL) calibration is used.

III. MEASUREMENT SETUP

A. COLON PHANTOM WITH POLYPS

The colon is the last part of the gastrointestinal tract. It has a segmented appearance due to a series of folds called haustra, and it is approximately 1,500 mm long and 40-90 mm in diameter. Polyps are slow-growing overgrowths of the colonic mucosa protruding into the lumen. When a colonoscopy is performed, the colon lumen is expanded using carbon dioxide insufflation. To model a colon during colonoscopy, we built a phantom with the anatomical and electrical properties of an expanded human colon. Our phantom is composed of a colon lumen model made of expanded polystyrene 268 mm in length and 66.7 mm in diameter, as shown in Fig. 4. The colon lumen was placed in the center of a cylindrical methacrylate container that was 300 mm in length and 150 mm in diameter. Expanded polystyrene has the same dielectric properties as air, making it an excellent model for the colon lumen. The polystyrene surface is undulated to simulate colon haustra and contains 4 holes to place polyps at different positions. The space between the colon lumen model and the external container walls is filled with a gelatin-oil mixture mimicking the dielectric properties of healthy mucosa tissue. The polyp is composed of a gelatin-oil mixture mimicking the dielectric properties of an adenomatous polyp with high-grade dysplasia (HGD) tissue [18].

The recipe for the healthy colon mucosa and high-grade dysplasia polyps was adapted from oil-gelatin phantoms developed for breast phantoms [24]. Oil-gelatin phantoms are low-cost, easy to produce, and nontoxic, and it is easy to change their dielectric properties by modifying the proportion of oil and water. In this case, we increased the amount of water to produce the high dielectric properties of healthy colon mucosa and polyps. In addition, some steps have been added to the original protocol [24] to produce large, high quality batches of material. First, the gelatin was hydrated with cold deionized water to completely dissolve the gelatin and

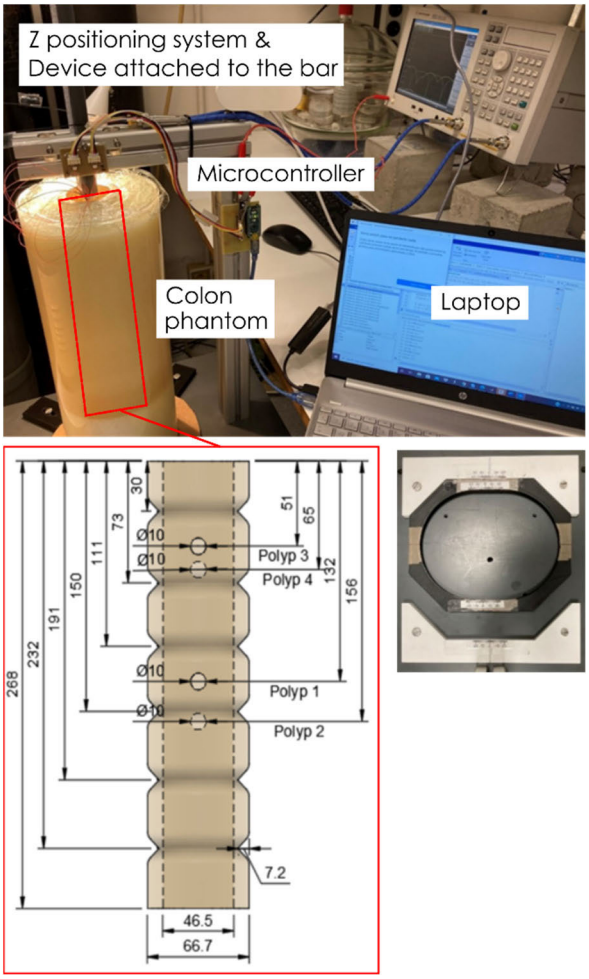

FIGURE 4. Measurement setup. The acquisition device is attached to the tip of a plastic bar. The colon phantom was placed on a 3D positioning system. The colon phantom was composed of tissue-mimicking materials poured in a methacrylate cylindrical box and an expanded polystyrene colon lumen model. The external microwave transceiver, controlling and processing unit was composed of a vector network analyzer (VNA), a microcontroller, and a laptop.

improve the homogeneity of the final mixture. To increase the velocity of polymerization and avoid the deposition of solids, the mixture was stirred continuously in a cold water bath until their temperature fell to 29 °C. Then the healthy mucosa material was poured into the phantom container between the container walls and the colon lumen polystyrene model until the container was completely filled avoiding the air gaps. Finally, the container was hermetically sealed with a silicone lid to avoid dehydration. The polyp material was poured in a small plastic airtight container. Both materials were stored in a refrigerator until they were completely solid. Before each use of the phantom, we extracted a spherical portion of 10 mm of polyp material and introduced it into the hole of the colon lumen polystyrene model. After each use, the phantom was stored in a refrigerator and completely sealed. The composition of the phantom mixtures is summarized in Table 2. No preservatives were added.

TABLE 2. Composition of the phantom mixtures.

Ingredient	Healthy mucosa	Polyp
Deionized water (ml)	3260.76	108.12
Gelatin 250 bloom (g)	326.62	10.83
Sunflower oil (ml)	1221.43	20.40
Dishwasher liquid (ml)	182.76	6.06

The dielectric properties of the tissue-mimicking phantoms were measured using the Keysight N1501A Dielectric slim form Probe Kit with the N1500A Materials Measurement Software Suite connected to a vector network analyzer Keysight E5071C. The dielectric properties of the phantom were measured before each use to track any degradation. The healthy mucosa phantom remained stable over the 30 days in which the explorations were performed, whereas the polyp phantom was redone every 15 days. The preservation of large batches of material without air contact was much longer than the preservation of the same material in smaller containers and with an air contact surface. Fig. 5 presents the relative permittivity and conductivity of the tissue-mimicking phantoms corresponding to healthy colon mucosa and polyps with high grade-dysplasia between 5-10 GHz. The dielectric properties of the phantom are compared to the measured dielectric properties of the corresponding human tissues by Guardiola *et al.* [18] and the dielectric properties of healthy colons from the IT'IS Database [25]. It can be observed that the dielectric properties of the tissue-mimicking materials reproduce both the contrast between the relative permittivity and the conductivity of the human tissue dielectric properties at 7.6 GHz.

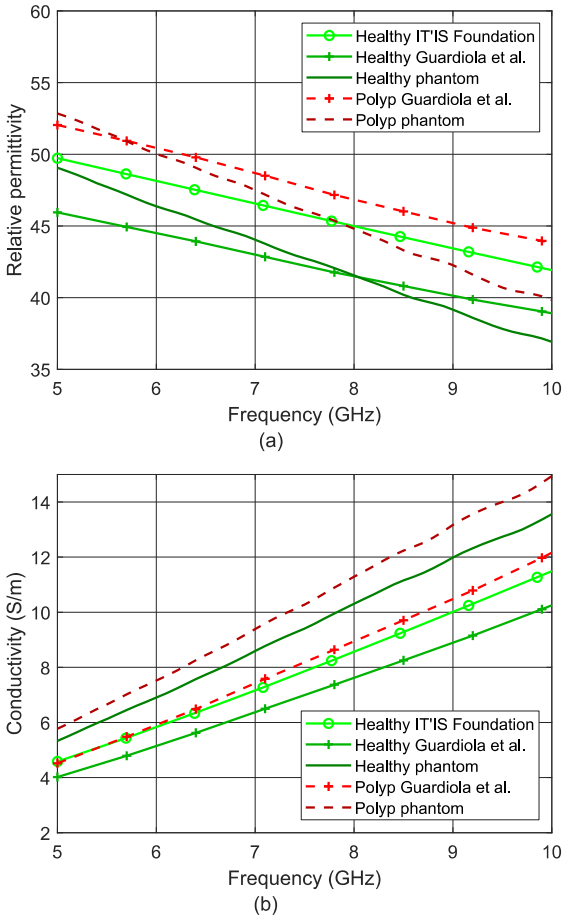

FIGURE 5. Measured dielectric properties of the phantom compared to the real patient tissues over the frequency. Polyps are unhealthy targets, and the colon mucosa is healthy tissue: (a) Relative permittivity; (b) Conductivity.

B. MEASUREMENT SETUP

To be able to reproduce a realistic colonoscopy exploration while the position of the acquisition device is known, a 3D positioning system was built (see Fig. 4). The measurement setup is composed of an L-shaped metallic structure fixed on a plastic base. The metallic structure holds a plastic bar equipped with a ruler. The acquisition device is then attached at the tip of the plastic bar. With this bar, the device is introduced vertically inside the colon lumen model. The colon phantom is placed on a mobile platform that allows movement along the x and y directions, while the plastic bar vertically allows movement of the acquisition device along the z direction. In this way, a complete positioning system in three dimensions is achieved, enabling any trajectory inside the colon phantom to be performed.

IV. DETECTION ALGORITHM

Microwave imaging is based on illuminating the object under test, the phantom, with incident radiation, E^i, and measuring the total received fields, E^t, resulting from the interaction of the incident radiation and the body under test. Data for the imaging are obtained by scanning the object from all directions. The total received field is the superposition of the incident field and the scattered field, E^s, which contains the information of the spatial changes of the dielectric properties of the phantom. By processing the total field with an imaging algorithm, the dielectric property contrast of the phantom can be reconstructed.

A. ACQUISITION ALGORITHM

Prior to the measurement, the VNA was calibrated up to the point of antenna feeding connection. The standard VNA calibration system including open-short-load connections was adopted. Since the acquisition device will be provided as a disposable set that includes the antenna array, the switching network and the cables, the VNA calibration only eliminates the effects of the VNA. Hence, the effect of slim and long coaxial cables remains and reduces the efficiency of the system. The software is a MATLAB code running on a laptop that performs 5 steps: i) establishes the connection between the VNA and the microcontroller and configures the measurement (bandwidth of 350 MHz, $N_f = 801$ frequency points, transmitting power of -5 dBm), ii) selects one transmitting and one receiving antenna pair, iii) sends the transmitting and receiving antenna selection code to the

TABLE 3. Trajectory characteristics.

#	Polyp	Num. frames	Description
1	3	49	Uniform, in front of polyp $x_i = 0, y_i = -8$
2	3	49	Uniform, further from polyp $x_i = 0, y_i = -6$
3	3	45	Uniform, further from polyp $x_i = 0, y_i = -3$
4	2	27	Uniform, centered $x_i = y_i = 0$
5	3	49	Uniform, centered $x_i = y_i = 0$
6	3	44	Uniform, centered $x_i = y_i = 0$
7	3	49	$x_i = y_i$ varying
8	3	49	Uniform, centered $x_i = y_i = 0$ with attenuators (32 dB)

microcontroller, iv) sends a trigger signal to the VNA to start the measurement of the transmitting coefficient between active antennas along the selected frequency band, v) reads the measured data from the VNA, vi) repeats ii-v until the data from all the antenna combinations are measured, vii) moves the acquisition device to the next position of the trajectory using the positioning system to obtain data from the next colon cross-section. The collected data is then stored for processing. In total, 24 combinations of transmission S-parameters (S21) are measured for each step of the trajectory. These combinations are obtained by alternatively selecting for each transmitting antenna the three closest receiving antennas, which are the adjacent, antenna and the two diagonal antennas.

To simulate a colonoscopy with the phantom, we have taken as a reference a real colonoscopy trajectory [26]. A trajectory refers to the (x, y, z) coordinates of the centroid of the acquisition cylindrical device, where the XY-plane is a horizontal or cross-sectional plane of the colon lumen, and z is the vertical coordinate. The origin of coordinates (0, 0, 0) is defined when the device is situated at the center of the cross-sectional plane of the colon lumen and the center of the 2 antenna rings is at the same height as the top base of the colon lumen (see Fig. 6). Each step of the trajectory is called a frame, $E^t_{z_i}(\vec{r}, f)$, where i is the index of the current frame. Each frame of the trajectories is separated 4 mm from the subsequent frame along the z-axis. For each frame, a $N_a \times 3 \times N_f$ matrix is obtained, where $\vec{r} = (x, y)$ and $N_a = 8$ is the number of transmitting and receiving antennas. In this study, eight different trajectories in the colon phantom with a 10-mm pedunculated polyp with HGD were measured. Table 3 summarizes the main trajectory characteristics.

B. IMAGING ALGORITHM

For each step of the trajectory, the following steps are conducted: i) calibrate the data to remove any error due to the movement of the device and the colon wall effect, ii) focus the data to obtain the reconstructed image of the dielectric contrast profile, iii) evaluate the threshold to identify whether or not there is a polyp, iv) repeat i-iii for each step of the trajectory, and v) calculate the overall sensitivity and specificity of the detection algorithm for the trajectory. The reconstruction has been done at a single frequency of $f = 7.6$ GHz.

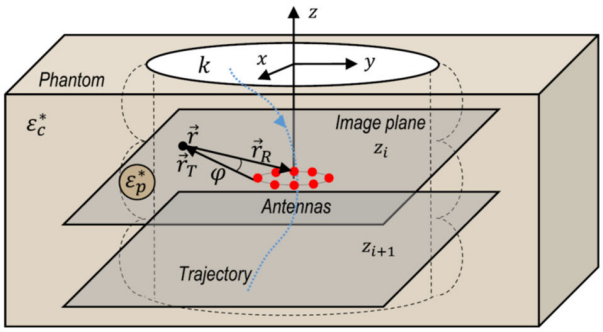

FIGURE 6. Trajectory described by the antenna array along the colon phantom.

1) CALIBRATION

Calibration consists of isolating solely the scattered field from the polyp, therefore removing any other effect. In our case, the main effect that contaminates the desired signal is the movement of the device and the colon, and thus the effect of having the colon wall at unknown and varying distances. We propose three calibration methods that share the same principle: subtraction from the actual measured frame, a previous measurement frame or a combination of previous measurement frames. The ideal calibration consists of subtracting the scattered field measured in a phantom with a polyp and its healthy counterpart, that is, a measurement with the same phantom but without polyps. In a real situation, this type of calibration is unfeasible because the healthy version of the actual colon under test is not available.

The first calibration approach is called Healthy Average Temporal (HAT) subtraction. This calibration consists of calculating the average of the transmission coefficient matrices corresponding to healthy frames, $E^t_{z_{h,j}}(\vec{r}, f)$, and subtracting it from the current measurement frame, $E^t_{z_i}(\vec{r}, f)$. This is possible in phantom experiments because there is prior knowledge of where the polyp is, but it is not feasible in clinical settings.

$$E^s_{z_i,HAT}(\vec{r}, f) = E^t_{z_i}(\vec{r}, f) - \sum_{j=1}^{N_h} \frac{1}{N_h} E^t_{z_{h,j}}(\vec{r}, f) \tag{1}$$

where N_h is the number of healthy steps averaged.

The second calibration approach is called Average Total (AT) subtraction and consists of averaging all the trajectory measurement steps and subtracting them from each measurement frame. This method is based on the hypothesis that in a colonoscopy, the vast majority of frames are healthy.

$$E^s_{z_i,AT}(\vec{r}, f) = E^t_{z_i}(\vec{r}, f) - \sum_{i=1}^{N_z} \frac{1}{N_z} E^t_{z_i}(\vec{r}, f) \tag{2}$$

where N_z is the total number of steps.

The last method is called the Hop and N Average Temporal (HNAT) subtraction. The idea behind this method is to skip the N closest frames to the current frame. The reason to skip frames from the calibration is to avoid including the effect

of the polyp if N is chosen conveniently. In this case, the scattered field produced by the polyp is estimated as:

$$E^{s}_{z_i,HNAT}(\vec{r},f) = E^{t}_{z_i}(\vec{r},f) - \sum_{j=i-H}^{i-H-N} \frac{1}{N} E^{t}_{z_j}(\vec{r},f) \tag{3}$$

where H is the number of steps that includes the leap and N is the number of steps that are averaged.

2) FOCUSING

Due to the small distances between the antennas and the colon wall, the information captured by the antennas is from a narrow region around the antennas. Therefore, a two-dimensional electromagnetic analysis can be performed. Considering the constraints of the system, two versions of a frequency domain imaging algorithm are implemented, namely, Bifocusing (B) and Modified Monofocusing (MM); see equations (4) and (5), respectively. These algorithms form every image point of the dielectric property contrast of the colon by creating one or two focused groups of antennas (one for the transmitters and the other for the receivers). The received scattered field from each antenna pair is numerically weighted with a focusing operator in order to be focused on a unique point in the reconstruction grid. The focusing operator restores the module and phase changes suffered by a wave on its way to and/or from every image point. For each image point, the coherent summation of all the scattering focused fields from all antenna combinations results in a large intensity value if the actual point is the origin of the scattering (polyp). If not, the summation results in a small value, and this contribution can be considered noise. Note that we assumed that the z-coordinates of the transmitting and receiving rings of antennas are the same; thus, their positions are denoted as $\vec{r}_T = (x_T, y_T)$ and $\vec{r}_R = (x_R, y_R)$, respectively.

$$I^{B}_{z_i}(\vec{r}) = \left| \sum_{k=(j-1)_{N_a}}^{(j+1)_{N_a}} \sum_{j=1}^{N_a} \frac{E_s(\vec{r}_{T_j}, \vec{r}_{R_k}, z_i)}{k^2 H_0^2(k\,|\vec{r}_{T_j} - \vec{r}|) H_0^2(k\,|\vec{r}_{R_k} - \vec{r}|)} \right| \tag{4}$$

$$I^{MM}_{z_i}(\vec{r}) = \left| \sum_{k=(j-1)_{N_a}}^{(j+1)_{N_a}} \sum_{j=1}^{N_a} E_s^2\left(\vec{r}_{T_j}, \vec{r}_{R_k}, z_i\right) J_1^2 \times \left(k\,|\vec{r}_{R_k} - \vec{r}|\right) e^{j2(k|\vec{r}_{R_k} - \vec{r}| + \varphi)} \right| \tag{5}$$

where $k = 2\pi f$ is the wavenumber and φ is the angle between the transmitting and receiving antennas.

3) THRESHOLDING

For each reconstructed image frame, $I_{z_i}(\vec{r})$, the thresholding method compares the maximum of the current reconstruction with the average maximum of the previous reconstructed images that have been classified as healthy, $I_{z_{h,j}}(\vec{r})$. If the quotient of those values is higher than the detection threshold, then the current frame is labeled as containing a polyp (6). Otherwise, the current frame is labeled as healthy and is added to the average of the healthy maximums. The first frame is always considered as healthy. For the frames labeled as containing a polyp, the system will generate an alarm.

$$\max\left\{I_{z_i}(\vec{r})\right\} \Big/ \sum_{j=1}^{N_h} \frac{1}{N_h} \max\left\{I_{z_{h,j}}(\vec{r})\right\} > \text{threshold} \tag{6}$$

Finally, the overall performance of the system to detect polyps in all trajectories is evaluated using the sensitivity and specificity. The sensitivity, also called the true positive (TP) rate, measures the percentage of cases having a polyp that are correctly diagnosed as having the lesion. A false negative (FN) occurs when a negative result is reported to a trajectory that does have a polyp. The specificity, also called the true negative (TN) rate, measures the percentage of healthy cases that are correctly identified as not having any polyp. A false positive (FP) is reported when the test wrongly indicates that a polyp is present. The values of sensitivity and specificity are related to the TP, FP, TN, and FN values through the following equations:

$$\text{sensitivity} = \frac{TP}{TP + FN} \tag{7}$$

$$\text{specificity} = \frac{TN}{TN + FP} \tag{8}$$

V. RESULTS

We measured and reconstructed the eight trajectories described in Table 3 using the different calibration methods. As an example, Fig. 7 shows the evolution of the normalized maximum amplitude of the reconstructed image registered in each step of the trajectory. The trajectories analyzed in Fig. 7 correspond to Trajectory 1 and Trajectory 7, where the polyp is between frames [44, 47] and [41, 44], respectively. The raw measured transmission coefficients for each antenna combination were calibrated using three different strategies: Average Total subtraction, Hop and N Average Temporal subtraction and Healthy Average Temporal subtraction. These will now be referred to as AT, HNAT and HAT, respectively. The first two strategies intend to emulate the results of the HAT, which is an ideal and non-realistic calibration. For each calibration strategy, the image was created using both Bifocusing and Modified Monofocusing focusing algorithms. The movement along the y-axis of the device, or the distance to the polyp, has also been included in the plots to analyze the relation between the device's displacement and the reconstruction. Vertical continuous orange lines indicate the limits of colon haustrum, and vertical continuous red lines indicate the limits of the polyp.

The maximum reconstructed amplitude represented in Fig. 7 has been normalized between 0 and 1, using the maximum amplitude of each calibration set, in order to enable a better comparison between the different methods and trajectories. It is possible to appreciate that the evolution of the maximum registered along the trajectory reveals an identical tendency for the three different calibration strategies and for

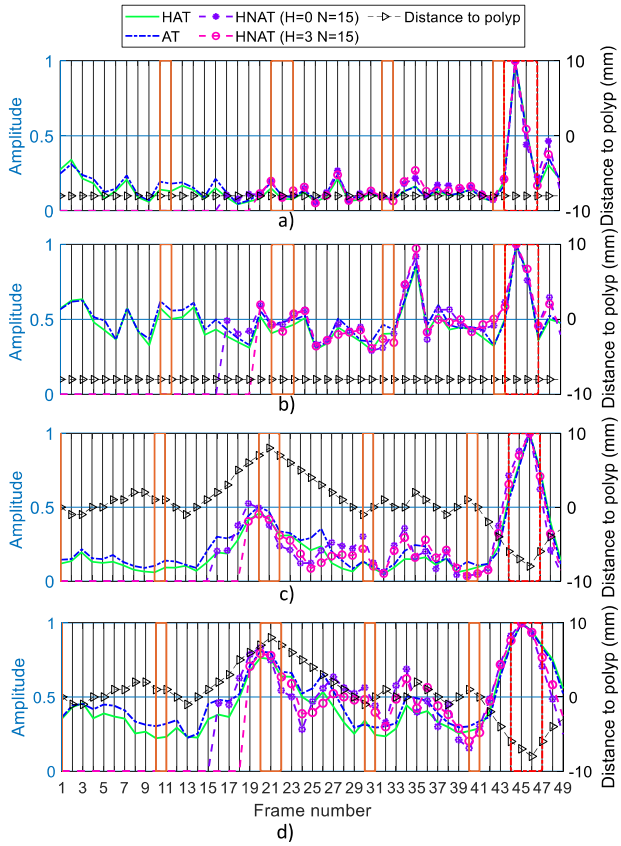

FIGURE 7. Evolution of the normalized maximum reconstructed amplitude for different calibrations: a) Trajectory 1 using Modified Monofocusing; b) Trajectory 1 using Bifocusing; c) Trajectory 7 using Modified Monofocusing; and d) Trajectory 7 using Bifocusing algorithm.

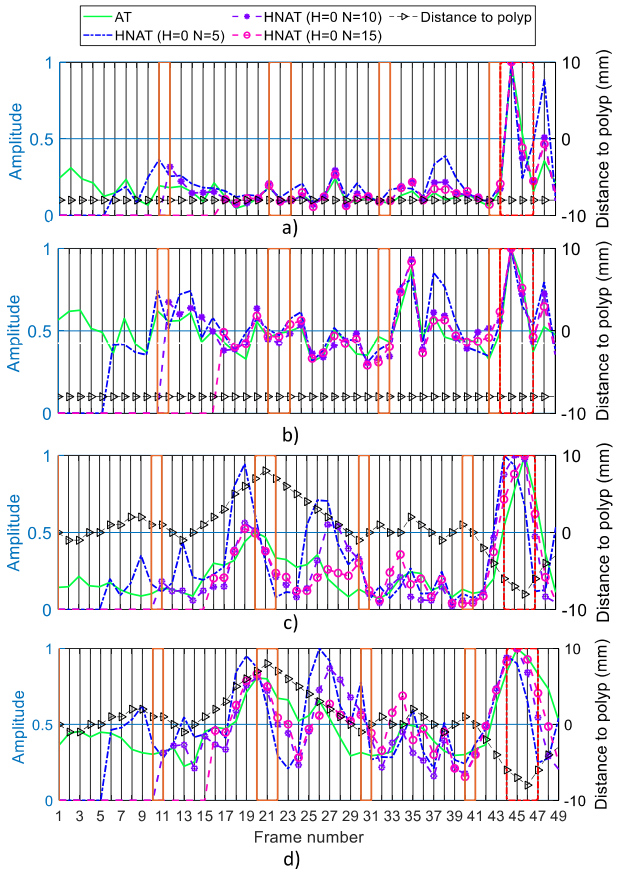

FIGURE 8. Evolution of the normalized maximum reconstructed amplitude for HNAT calibration using different N and H parameters: a) Trajectory 1 using Modified Monofocusing; b) Trajectory 1 using Bifocusing; c) Trajectory 7 using Modified Monofocusing; and d) Trajectory 7 using Bifocusing algorithm.

the two focusing algorithms, i.e., Modified Monofocusing and Bifocusing. Indeed, the absolute maximum of all the traces displayed in Fig. 7 corresponds to the position of the polyp. Local maximums are also observed when the trajectory approaches the colon walls. Haustrum does not seem to produce any effect on the reconstructed results.

Concerning the calibration strategies, both AT and HNAT offer a similar performance to HAT. In the case of the HNAT strategy, the number of averaged frames (N) is set to 15, and two different sizes of the backwards leap (H) are analyzed. On one hand, H has been assigned a value of 3 since polyp diameter is always 10 mm; therefore, there are only 4 frames in which the polyp is inside the detection zone of the device. Hence, if we want to avoid including information from the polyp in the calibration set, it is necessary to omit the 3 previous frames to the frame that is actually reconstructed. Likewise, the case of $H = 0$ has also been analyzed to assess whether a sufficiently large number of averaged frames (N) could minimize the effect of the polyps during the calibration, thereby emulating the principle of the AT strategy. Fig. 8 includes the results obtained when calibrating with different N values and H=0. As shown in Fig. 8, the larger N is, the less sensitive the calibration is to noise and therefore the more robust it is. Additionally, in the frames where the polyp is detected, a larger N minimizes the contribution of the polyp in the average used to calibrate, allowing a more similar detection to the one observed with the AT strategy.

Regarding the focusing method, as shown in Fig. 7, the difference in amplitude between the frames that correspond to a healthy colon and those where the polyp is inside the detection zone of the device is higher when Modified Monofocusing algorithm is used, allowing an easier detection of the polyp using a threshold without false positives. Fig. 9 shows the cross-sectional reconstructed images using AT calibration and Modified Monofocusing and Bifocusing algorithms in the frame corresponding to the absolute maximum in Fig. 7; that is, the position of the polyp. The magnitude represented is the normalized reconstructed dielectric contrast profile at 7.6 GHz represented on a logarithmic scale between 0 and 1. The blue circle in the middle of the plots indicates the position of the device, and the red dots indicate the position of each antenna. As shown in Fig. 9, both algorithms are able to detect and locate the polyp, showing higher intensities in the position of the polyp. The Modified Monofocusing algorithm can obtain punctual

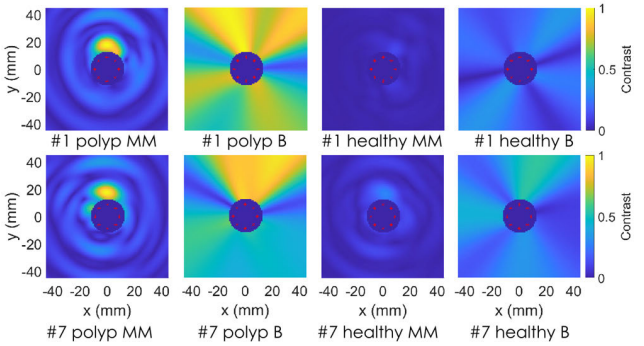

FIGURE 9. Cross-sectional reconstruction of the normalized dielectric contrast corresponding to Trajectories 1 and 7 for the frame that contains the absolute maximum amplitude of the trajectory (polyp) and a healthy frame using Bifocusing (B) and Modified Monofocusing (MM). The calibration was performed with the AT strategy.

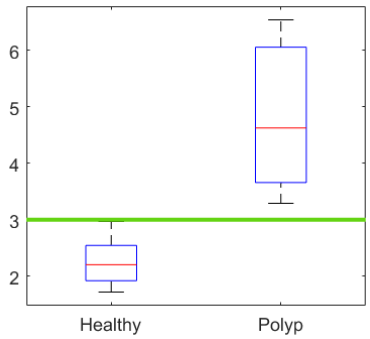

FIGURE 10. Normalized maximum reconstructed amplitude of each patient and frame for healthy mucosa and for polyps using Modified Monofocusing and HNAT. The detection threshold is represented as a green line.

detection, while Bifocusing does not obtain discrimination in the range direction.

Finally, we assess the performance of the complete detection algorithm. Seeing the previous results, we selected Modified Monofocusing as the focusing algorithm and HNAT as the calibration method. The values of N and H were selected depending on the characteristics of each trajectory. Fig. 10 shows a boxplot that represents the normalized maximum reconstructed amplitude of each patient and frame for healthy mucosa and for polyps. The blue box includes the values within the 25^{th} and 75^{th} percentiles and the red line is the median. The detection threshold is represented as a horizontal green line. All the values above the threshold were classified as lesions and those below as healthy mucosa. The detection thresholds were defined to optimize the specificity and sensitivity to detect polyps from healthy mucosa. True detection is considered when the maximum amplitude of a frame is higher than the threshold in at least one frame, and this frame is within the range of frames where the polyp is in front of any antenna. The results show that Modified Monofocusing combined with HNAT provides a perfect detection, fixing the threshold to 3 without false positives or false negatives. This means a specificity and sensitivity equal to 100% and ensures that no polyps are missed.

VI. DISCUSSION AND CONCLUSION

We evaluated a novel microwave-based device and used the IDEAL model to drive this innovation. In this paper, we reported on the process of conceptualization and preparation before its implementation in patients. The IDEAL Framework and Recommendations [27] represent a new paradigm for evaluating surgical operations, invasive medical devices and other complex therapeutic interventions. A miniaturized acquisition system for a microwave colonoscopy system to detect colorectal polyps with an alarm was presented in this paper. The acquisition device was designed as a switched cylindrical array of 16 antennas organized in two rings of eight antennas, each containing the transmitters and the receivers. The device was encapsulated and attached at the tip of a bar simulating a colonoscope. The antennas were switched in pairs following a predefined sequence, and the S-parameters were measured to obtain a measured frame. This process was repeated a number of steps to form a trajectory. A vector network analyzer, a microcontroller and a laptop were used for data acquisition and signal processing.

The system was designed to be compatible with colonoscopy and produce minimal changes into current clinical practice. First, concerning size restrictions, the final dimensions of the acquisition device are 30 mm in length by 20 mm in diameter, with a total thickness of 3 mm. The dimensions and shape of the device ensure non-obstruction of the front tip of the colonoscope, avoids injuring the patient or hindering the maneuverability of the colonoscope. Similar accessories in shape and size are available on the market, and in the future the accessory could be integrated into the colonoscope tube. The antenna elements show typical electrically small antenna performance, characterized by a narrow bandwidth of 60 MHz (0.8% fractional bandwidth) and an omnidirectional radiation pattern. An omnidirectional radiation pattern is suitable for this case, where we want to ensure a 360° coverage of the colon wall. Mutual coupling between adjacent antennas has been minimized to −13 dB using cavity-backed antenna design.

The system is verified with a colon phantom that simulates realistic colonoscopy exploration. The phantom models a section of a colon, including the haustrum and allows placement of different polyps. The phantom is composed of gelatin-oil based materials to mimic the dielectric properties of colon healthy mucosa and polyps with high-grade dysplasia. Once manufactured, the tissue-mimicking materials were measured with a coaxial probe, achieving dielectric properties very similar to those of real human tissues, with relative permittivities of 41 and 46 and conductivities of 9 S/m and 9.8 S/m, respectively.

The acquired data are processed with a 3-step algorithm that generates an alarm when a polyp is detected. In the first step, the scattering fields are estimated by using three different calibration methods. This is a crucial step to remove the spatial-temporal uncertainty on the reception of the scattered fields due to the unknown and changing distance

from the acquisition device and the colon wall. Next, two focusing methods are compared to obtain a cross-sectional image of each step, and finally a detector based on a threshold is used to generate the alarm.

Regarding the calibration, the most important challenge is to differentiate the effect of the device and the colon movements from the effect of the presence of the polyp, since both produce changes in the measured scattered field. This can be observed if we compare the results of Trajectory 1 and Trajectory 7 in Fig. 7. Trajectory 7 shows a smaller difference between the absolute and local maximums, suggesting that the main undesired effect that the calibration must face is device movement. This effect is evident in frames 15 to 22 of Trajectory 2; in this region, the accessory moves along the y-axis toward the colon wall. Thus, the device movement is not completely corrected with any calibration; however, the correction obtained is sufficient to achieve perfect detection of polyps in the studied cases. AT and HNAT offer a similar performance to HAT. Hence these two strategies can be used to simulate the HAT, which although it is the ideal calibration, it is unrealistic since it depends on prior knowledge of healthy frames, which is knowledge that is not available in a clinical scenario. AT offers similar results to HAT if the percentage of frames with polyp vs. healthy frames is less than 10%. HNAT seems to be the most suitable calibration in a real case, even though the first $N+H$ frames cannot be calibrated nor analyzed. Moreover, the selection of N values is a key, as the larger N is, the better the results, but the greater the calibrated detection is delayed. In this paper, the selection of these values was performed manually; however, in a realistic scenario it must be done automatically. To do so, more trajectories in phantoms of different shapes will be studied.

Regarding the focusing method, Modified Monofocusing presents better results while avoiding false positives in regions with large movements. Moreover, Modified Monofocusing presents focused detection with fewer artifacts, whereas Bifocusing is only able to focus on an angular section. The main reason for this lack of range resolution is the narrow frequency band of the antennas. However, this is not a problem for our system since the output is only an alarm. According to the opinion of more than 30 doctors with whom we have collaborated, it is not necessary for our device to provide additional information, for example, the angular position of the polyp, since it could distract the doctor's attention during colonoscopy. The unusual imaging configuration in which the antennas are surrounded by the imaging region (colon) causes there to be no direct vision between half of the array antennas and the focusing point since the signal cannot pass through the device. For this reason, focusing based on re-establishing the effect produced in the fields due to the distance between an image point and the transmitting and receiving antennas is wrong for these antenna combinations. This effect has been reduced by only including the three closest receiving antennas for each transmitter in the reconstruction. The residual error produced by this effect is translated into artifacts in the reconstructed image, especially appearing with the Bifocusing method. Moreover, due to the narrowband behavior of the antennas, we cannot benefit from a frequency averaging, which is commonly used to cancel the frequency selective artifacts [28].

Finally, it has been observed that it is possible to define a fixed threshold that would enable perfect detection of the polyp in all of the studied trajectories. Notwithstanding, more trajectories must be tested, and more sophisticated thresholding methods will be designed to make the threshold more robust.

Eight different trajectories were measured to assess different detection challenges of this application:

1) The phantom includes six folds to study the effect of colon folds. We have shown that the folds do not produce false positives in any of the trajectories made with this phantom.
2) Two polyp positions were considered: Polyp 2 was in between colon folds, and Polyp 3 was just behind a fold. A polyp behind a fold is difficult to detect with conventional colonoscopy because the camera only has frontal vision. We demonstrated with Trajectory 4 that a polyp behind a fold can be detected.
3) The movement of the colonoscope, and hence the unknown distance between the antenna and the colon, was studied with Trajectory 7. We demonstrated that the developed calibration is able to reduce this effect to allow detection.
4) Repeatability. Three uniform and centered trajectories (4, 5, 6) were performed, and we obtained very similar results.
5) Attenuation. We studied the capacity to detect polyps at different distances with Trajectories 1, 2, and 3. In Trajectory 8, we included 16 dB attenuators between the VNA ports and the coaxial cable. Therefore, with a total additional attenuation of 32 dB detection is still possible. The reason to do so is to simulate the losses expected for the 2 m coaxial cables that will be used in the final system.

The main limitation of this study is that the phantom does not include angulations. The ability to detect polyps of different sizes and shapes (sessile and flat) has also not been studied. Therefore, further studies with a colon lumen model extracted from patient computed tomography colonography will be manufactured, measured and reconstructed in future experiments.

In summary, this study demonstrated for the first time the use of a microwave-based device to be used as an accessory of a standard colonoscope to detect polyps in a phantom.

REFERENCES

[1] J. Ferlay, M. Ervik, F. Lam, M. Colombet, L. Mery, M. Piñeros, A. Znaor, I. Soerjomataram, and F. Bray, "Global cancer observatory: Cancer today," Int. Agency Res. Cancer, Lyon, France, 2020. Accessed: Jul. 28, 2021. [Online]. Available: https://gco.iarc.fr/today
[2] R. L. Siegel, K. D. Miller, and A. Jemal, "Cancer statistics, 2015," *CA Cancer J. Clin.*, vol. 65, no. 1, pp. 5–29, 2015.

[3] (2021). *Surveillance Research Program, National Cancer Institute SEER*Stat Software*. [Online]. Available: seer.cancer.gov/seerstat

[4] J. C. van Rijn, J. B. Reitsma, J. Stoker, P. M. Bossuyt, S. J. van Deventer, and E. Dekker, "Polyp miss rate determined by tandem colonoscopy: A systematic review," *Amer. J. Gastroenterol.*, vol. 101, no. 2, pp. 343–350, 2006.

[5] N. J. Samadder, K. Curtin, T. M. Tuohy, L. Pappas, K. Boucher, D. Provenzale, K. G. Rowe, G. P. Mineau, K. Smith, R. Pimentel, and A. C. Kirchhoff, "Characteristics of missed or interval colorectal cancer and patient survival: A population-based study," *Gastroenterology*, vol. 146, no. 4, pp. 950–960, 2014.

[6] W. N. Sing and C. Rees, "Can technology increase adenoma detection rate," *Therapeutic Adv. Gastroenterol.*, vol. 11, pp. 1–18, Jan. 2018.

[7] R. Kumashiro, K. Konishi, T. Chiba, T. Akahoshi, S. Nakamura, M. Murata, M. Tomikawa, T. Matsumoto, Y. Maehara, and M. Hashizume, "Integrated endoscopic system based on optical imaging and hyperspectral data analysis for colorectal cancer detection," *Anticancer Res.*, vol. 36, no. 8, pp. 3925–3932, 2016.

[8] G. Urban, P. Tripathi, T. Alkayali, M. Mittal, F. Jalali, W. Karnes, and P. Baldi, "Deep learning localizes and identifies polyps in real time with 96% accuracy in screening colonoscopy," *Gastroenterology*, vol. 155, no. 4, pp. 1069–1078.e8, 2018.

[9] J. E. East, B. P. Saunders, D. Burling, D. Boone, S. Halligan, and S. A. Taylor, "Surface visualization at CT colonography simulated colonoscopy: Effect of varying field of view and retrograde view," *Amer. J. Gastroenterol.*, vol. 102, no. 11, pp. 2529–2535, Nov. 2007.

[10] D. Freedman, Y. Blau, L. Katzir, A. Aides, I. Shimshoni, D. Veikherman, T. Golany, A. Gordon, G. Corrado, Y. Matias, and E. Rivlin, "Detecting deficient coverage in colonoscopies," *IEEE Trans. Med. Imag.*, vol. 39, no. 11, pp. 3451–3462, Nov. 2020.

[11] N. K. Nikolova, *Introduction to Microwave Imaging*. Cambridge, U.K.: Cambridge Univ. Press, 2017.

[12] P. M. Meaney, D. Goodwin, A. H. Golnabi, T. Zhou, M. Pallone, S. D. Geimer, G. Burke, and K. D. Paulsen, "Clinical microwave tomographic imaging of the calcaneus: A first-in-human case study of two subjects," *IEEE Trans. Biomed. Eng.*, vol. 59, no. 12, pp. 3304–3313, Dec. 2012.

[13] S. Y. Semenov, V. G. Posukh, A. E. Bulyshev, T. C. Williams, Y. E. Sizov, P. N. Repin, A. Souvorov, and A. Nazarov, "Microwave tomographic imaging of the heart in intact swine," *J. Electromagn. Waves Appl.*, vol. 207, no. 7, pp. 873–890, 2006.

[14] M. Shere, I. Lyburn, R. Sidebottom, H. Massey, C. Gillett, and L. Jones, "MARIA m5: A multicentre clinical study to evaluate the ability of the micrima radio-wave radar breast imaging system (MARIA) to detect lesions in the symptomatic breast," *Eur. J. Radiol.*, vol. 116, pp. 61–67, Jul. 2019.

[15] D. O'Loughlin, M. O'Halloran, B. M. Moloney, M. Glavin, E. Jones, and M. A. Elahi, "Microwave breast imaging: Clinical advances and remaining challenges," *IEEE Trans. Biomed. Eng.*, vol. 65, no. 11, pp. 2580–2590, Nov. 2018.

[16] L. Crocco, I. Karanasiou, M. L. James, and R. C. Conceição, *Emerging Electromagnetic Technologies for Brain Diseases Diagnostics, Monitoring and Therapy*. Cham, Switzerland: Springer, 2018.

[17] O. Karadima, M. Rahman, I. Sotiriou, N. Ghavami, P. Lu, S. Ahsan, and P. Kosmas, "Experimental validation of microwave tomography with the DBIM-TwIST algorithm for brain stroke detection and classification," *Sensors*, vol. 20, no. 3, p. 840, 2020.

[18] M. Guardiola, S. Buitrago, G. Fernández-Esparrach, J. M. O'Callaghan, J. Romeu, M. Cuatrecasas, H. Córdova, M. Á. G. Ballester, and O. Camara, "Dielectric properties of colon polyps, cancer, and normal mucosa: *Ex vivo* measurements from 0.5 to 20 GHz," *Med. Phys.*, vol. 45, no. 8, pp. 3768–3782, Aug. 2018.

[19] W. S. Ngu, R. Bevan, Z. P. Tsiamoulos, P. Bassett, Z. Hoare, M. D. Rutter, G. Clifford, N. Totton, T. J. Lee, A. Ramadas, J. G. Silcock, J. Painter, L. J. Neilson, B. P. Saunders, and C. J. Rees, "Improved adenoma detection with endocuff vision: The ADENOMA randomised controlled trial," *Gut*, vol. 68, no. 2, pp. 280–288, Feb. 2019.

[20] A. Repici, M. Badalamenti, R. Maselli, L. Correale, F. Radaelli, E. Rondonotti, E. Ferrara, M. Spadaccini, A. Alkandari, A. Fugazza, A. Anderloni, P. A. Galtieri, G. Pellegatta, S. Carrara, M. Di Leo, V. Craviotto, L. Lamonaca, R. Lorenzetti, and C. Hassan, "Efficacy of real-time computer-aided detection of colorectal neoplasia in a randomized trial," *Gastroenterology*, vol. 159, no. 2, pp. 512–520, 2020.

[21] M. Klemm, I. J. Craddock, J. A. Leendertz, A. Preece, and R. Benjamin, "Radar-based breast cancer detection using a hemispherical antenna array—Experimental results," *IEEE Trans. Antennas Propag.*, vol. 57, no. 6, pp. 1692–1704, Jun. 2009.

[22] B. J. Mohammed, A. M. Abbosh, S. Mustafa, and D. Ireland, "Microwave system for head imaging," *IEEE Trans. Instrum. Meas.*, vol. 63, no. 1, pp. 117–123, Jan. 2014.

[23] M. Guardiola, K. Djafri, M. Challal, M. A. Gonzalez Ballester, G. Fernandez-Esparrach, O. Camara, and J. Romeu, "Design and evaluation of an antenna applicator for a microwave colonoscopy system," *IEEE Trans. Antennas Propag.*, vol. 67, no. 8, pp. 4968–4977, Aug. 2019.

[24] S. Di Meo, L. Pasotti, I. Iliopoulos, M. Pasian, M. Ettorre, M. Zhadobov, and G. Matrone, "Tissue-mimicking materials for breast phantoms up to 50 GHz," *Phys. Med. Biol.*, vol. 64, no. 5, Feb. 2019, Art. no. 055006.

[25] P. A. Hasgall *et al.*, "IT'IS database for thermal and electromagnetic parameters of biological tissues," May 2018. Accessed: Jul. 28, 2021. [Online]. Available: https://itis.swiss/virtual-population/tissue-properties/database/dielectric-properties/

[26] K. G. V. J. Jayender and R. S. J. Estepar, "New kinematic metric for quantifying surgical skill for flexible instrument manipulation," in *Proc. 1st Int. Conf. Inf. Process. Comput.-Assist. Intervent. (IPCAI)*, Geneva, Switzerland, Jun. 2010, pp. 81–90, doi: 10.1007/978-3-642-13711-2_8.

[27] *IDEAL Collaboration*. Accessed: Jul. 28, 2021. [Online]. Available: https://www.ideal-collaboration.net/

[28] L. Jofre, A. Broquetas, J. Romeu, S. Blanch, A. P. Toda, X. Fabregas, and A. Cardama, "UWB tomographic radar imaging of penetrable and impenetrable objects," *Proc. IEEE*, vol. 97, no. 2, pp. 451–464, Feb. 2009.

ALEJANDRA GARRIDO received the degree in engineering and the master's degree in telecommunications from the Universitat Politècnica de Catalunya, Barcelona. She has been working on microwave systems and antenna design, since 2018, as a part-time Research Assistant at Comsenslab (UPC). In 2018, she completed her stay at Aalto University, Finland, designing integrated antennas for green buildings. She is currently working as a Software Engineer with MiWEndo Solutions. She has coauthored four scientific articles. She has experience working in machine learning and computer vision.

ROBERTO SONT received the degree in telecommunications engineering and the master's degree in telecommunications from the Universitat Politècnica de Catalunya, Barcelona, in 2017 and 2019, respectively. He is currently a Hardware Engineer with MiWEndo Solutions. He has developed a measurement system for Zanini Auto Group to characterize radomes in the automotive sector as a final degree project.

WALID DGHOUGHI received the degree in biomedical engineering with a major in medical imaging and the M.Sc. degree in biomedical engineering from UPM, and the master's degree in technological innovation in health programme (EIT Health). He is highly enthusiast about technological innovation and a strong believer in the role of engineering in the progress of medicine. He is trained in innovation and entrepreneurship, AI, and eHealth.

SERGI MARCOVAL received the bachelor's degree in biomedical engineering from Universitat Pompeu Fabra, in 2021. In 2020, he performed an Erasmus Program at the Politecnico di Milano, Italy. He is passionate about medical devices, especially those related to minimally invasive diagnosis and therapies. He is currently working in preclinical validation and regulatory affairs with MiWEndo Solutions.

JORDI ROMEU (Fellow, IEEE) was born in Barcelona, Spain, in 1962. He received the Ingeniero de Telecomunicación and Doctor Ingeniero de Telecomunicación degrees from the Universitat Politècnica de Catalunya (UPC), in 1986 and 1991, respectively. In 1985, he joined the Antenna Laboratory, Signal Theory and Communications Department, UPC, where he is currently a Full Professor, and involved in antenna near-field measurements, antenna diagnostics, and antenna design. He was a Visiting Scholar with the Antenna Laboratory, University of California at Los Angeles, Los Angeles, in 1999, on a NATO Scientific Program Scholarship, and the University of California at Irvine, in 2004. He holds several patents and has published 60 refereed articles in international journals and 80 conference proceedings. He was the Grand Winner of the European IT Prize, awarded by the European Commission, for his contributions in the development of fractal antennas, in 1998 (more information can be found at http://www.researchgate.net/profile/Jordi-Romeu).

GLÒRIA FERNÁNDEZ-ESPARRACH received the M.D. degree from the University of Barcelona, in 1988, and the Ph.D. degree in 1997. She was a Diplomate of Spanish Board of Gastroenterology. She has been a Professor with the University of Barcelona, since 2015. With more than 20 years of experience in clinical practice as an Endoscopist at HCB, in the last ten years, she has focused her activity on therapeutic endoscopy and endoscopic ultrasonography. After a stay as a Guest Researcher at the Experimental Endoscopy Unit, Brigham and Women's Hospital, Boston, under the direction of Dr. Christopher C. Thompson, from July 2007 to June 2008, she started her own Experimental Endoscopy Laboratory, in 2009. She is currently a Researcher with IDIBAPS and CIBEREHD.

IGNASI BELDA is currently a Computer Scientist, a Doctor in artificial intelligence applied to drug discovery, and a Doctor in law and taxation. He has been the CEO of the Barcelona Science Park for two years. He has founded or co-founded six start-ups in biomedicine. He has published dozens of scientific articles, he has participated as a speaker in more than 50 international conferences and has written six outreach books about artificial intelligence and telecommunications, which have been translated into multiple foreign languages. Thanks to his entrepreneurship career, he has been awarded 20 national and international prizes, including the Award Princesa de Girona, in 2014, or the Headstart Catalyst Award, in 2020, given by the U.S. National Academy of Medicine.

MARTA GUARDIOLA has been working in microwave imaging systems for medical diagnosis with the Universitat Politècnica de Catalunya, since 2008, and the Universitat Pompeu Fabra, since 2014. She is currently an Engineer and a Doctor in telecommunications. She has authored six refereed articles in international journals and 25 conference proceedings. She holds a patent and was awarded ten prizes, including The Spinoff Prize, a Nature Research Award. Her research interests include microwave imaging algorithms, computational models and electromagnetic simulations, the design and manufacturing of microwave imaging acquisition systems, and preclinical validation.

sensors

MDPI

Article

MiWEndo: Evaluation of a Microwave Colonoscopy Algorithm for Early Colorectal Cancer Detection in Ex Vivo Human Colon Models

Marta Guardiola [1,*], Walid Dghoughi [1], Roberto Sont [1], Alejandra Garrido [1], Sergi Marcoval [1], Luz María Neira [1], Ignasi Belda [1] and Glòria Fernández-Esparrach [1,2]

[1] MiWEndo Solutions S.L., 08014 Barcelona, Spain; wdghoughi@miwendo.com (W.D.); rsont@miwendo.com (R.S.); agarrido@miwendo.com (A.G.); smarcoval@miwendo.com (S.M.); lmneira@miwendo.com (L.M.N.); ibelda@miwendo.com (I.B.); gfernan@miwendo.com (G.F.-E.)
[2] Endoscopy Unit, Gastroenterology Department, Hospital Clínic, University of Barcelona, 08036 Barcelona, Spain
* Correspondence: marta@miwendo.com

Abstract: This study assesses the efficacy of detecting colorectal cancer precursors or polyps in an ex vivo human colon model with a microwave colonoscopy algorithm. Nowadays, 22% of polyps go undetected with conventional colonoscopy, and the risk of cancer after a negative colonoscopy can be up to 7.9%. We developed a microwave colonoscopy device that consists of a cylindrical ring-shaped switchable microwave antenna array that can be attached to the tip of a conventional colonoscope as an accessory. The accessory is connected to an external unit that allows successive measurements of the colon and processes the measurements with a microwave imaging algorithm. An acoustic signal is generated when a polyp is detected. Fifteen ex vivo freshly excised human colons with cancer (n = 12) or polyps (n = 3) were examined with the microwave-assisted colonoscopy system simulating a real colonoscopy exploration. After the experiment, the dielectric properties of the specimens were measured with a coaxial probe and the samples underwent a pathology analysis. The results show that all the neoplasms were detected with a sensitivity of 100% and specificity of 87.4%.

Keywords: endoscopes; medical diagnostic imaging; microwave antenna arrays; microwave imaging; colorectal cancer

check for updates

Citation: Guardiola, M.; Dghoughi, W.; Sont, R.; Garrido, A.; Marcoval, S.; Neira, L.M.; Belda, I.; Fernández-Esparrach, G. MiWEndo: Evaluation of a Microwave Colonoscopy Algorithm for Early Colorectal Cancer Detection in Ex Vivo Human Colon Models. *Sensors* **2022**, *22*, 4902. https://doi.org/10.3390/s22134902

Academic Editor: Andrea Randazzo

Received: 30 May 2022
Accepted: 26 June 2022
Published: 29 June 2022

Publisher's Note: MDPI stays neutral with regard to jurisdictional claims in published maps and institutional affiliations.

Copyright: © 2022 by the authors. Licensee MDPI, Basel, Switzerland. This article is an open access article distributed under the terms and conditions of the Creative Commons Attribution (CC BY) license (https://creativecommons.org/licenses/by/4.0/).

1. Introduction

Colorectal cancer (CRC) is a major health and economic burden in the context of an increasingly aging population. Globally, 1.93 million new cases of CRCs are diagnosed each year, and 935,000 people died of CRCs in 2020 [1], making it the second most common cause of cancer death in both men and women. CRC is a malignant disease that affects the colon and rectum. Ninety percent of CRCs start as a polyp, i.e., an abnormal colon mucosa growth [2]. Although some polyps are harmless, the adenoma type is premalignant and slowly becomes cancerous. Since polyps are usually asymptomatic or present mild symptoms, CRC is commonly found in advanced stages [3]. The five-year survival rate is approximately 65%, but it strongly depends on the development stage at diagnosis, dropping to 14% if cancer has spread to distant parts of the body. Fortunately, early diagnosis can dramatically improve prognosis, saving lives and reducing healthcare costs.

To date, colonoscopy is the most effective diagnostic and therapeutic technique for preventing colorectal cancer since it allows the identification and removal of polyps in the entire colon. Several prospective studies demonstrate that colonoscopy with polypectomy reduces the incidence of CRC by 40–90% [4,5]. Nevertheless, colonoscopy is far from perfect: 22% of polyps go undetected [6], and cancer incidence after a negative colonoscopy is still 7.9% [7]. This lack of efficacy is mainly caused by visualization limitations, since the camera has a field of view of less than 180° [8], inhomogeneous illumination, colon

angulations and folds, and poor colon cleaning. For this reason, 13.4% of the colon surface area might not be visualized during a colonoscopy [9].

Several endoscopic devices and technologies have been developed to improve the adenoma detection rate (ADR). ADR is the quality indicator of colonoscopy, as each 1% increase in ADR decreases patients' risk of CRC by 3% [10]. High-definition endoscopes, endoscopes with multiple lenses, and mucosal flattening accessories [11,12] have demonstrated an increase in ADR of 4.5%, 5%, and 16%, respectively, by improving colon visualization [13]. Artificial intelligence for the real-time assessment of endoscopic images [14] has shown an increase in ADR of 14% [15]. However, if the camera does not visualize the adenoma, the algorithm cannot detect it. Chromoendoscopy, endoscopic microscopy (endocytoscopy and endomicroscopy), and hyperspectral techniques [16] are methods that have been developed to magnify and enhance mucosa tissue characteristics linked to malignancy, but have failed to demonstrate significant increases in ADR [13]. All these techniques are restricted to the optical information captured by the camera and require highly trained professionals. Their outcomes are highly dependent on the operator's experience and human factors like fatigue, stress, and resilience. Therefore, a tool capable of automatizing the detection of polyps is needed.

We recently proposed microwave imaging, a non-ionizing, anatomical, and functional imaging method [17] to detect polyps in the colon. Compared to advanced colonoscopy methods, microwave imaging offers a new contrast mechanism that is independent of the information captured by the optical camera. Microwave imaging retrieves the dielectric properties of a target—the relative permittivity and the conductivity—from the measured electromagnetic fields. The dielectric properties are biomarkers of several health conditions, such as breast cancer [18,19], brain stroke [20], osteoporosis [21], heart infarction [22], or edema. We demonstrated in an ex vivo study with human colon polyps and healthy mucosa that the dielectric properties of colon polyps increase when the malignancy grade increases. At 8 GHz, the contrast between healthy colon mucosa and colorectal cancer is 30% and 90% for the relative permittivity and conductivity, respectively [22]. We developed a prototype to integrate microwave imaging into conventional colonoscopy called MiWEndo. MiWEndo is a ring-shaped switchable antenna array accessory attachable to the distal tip of a standard colonoscope connected to an external processing unit. MiWEndo provides a field of view inside the colon of 360° and generates an acoustic signal when it detects a polyp in the microwave image [23]. A frequency-domain reconstruction scheme based on a modified back-projection method preceded by a calibration was developed to form cross-sectional images of the colon every 4 mm for each colon model. A fixed threshold was used to detect if a polyp was present in each image. A preliminary algorithm was tested in phantoms [24] and ex vivo models [25]. These studies concluded that the calibration and the detection steps had to be improved. In [26] we performed a comparative study between five different calibration methods to define the most suitable one.

In this paper we present an improved microwave colonoscopy algorithm for early colorectal cancer detection. This study aims to assess the overall algorithm performance with 15 freshly excised human colon specimens with neoplastic lesions. This algorithm uses the calibration scheme identified in [26] and an improved automatic detection method. The colon models were placed on a setup designed to emulate a colonoscopy exploration with the MiWEndo microwave-based colonoscopy system. The results were compared with the gold standard pathology analysis in terms of sensitivity and specificity. We also characterized the dielectric properties of the specimens at 7.6 GHz with an open-ended coaxial probe.

2. Materials and Methods

2.1. Microwave-Based Colonoscopy System

The imaging system is composed of an external processing unit and an acquisition accessory. The external unit contains a vector network analyzer (E5071C ENA VNA, Keysight, Santa Rosa, CA, USA), a microcontroller (Arduino Nano, Arduino, New York,

NY, USA), and a laptop. The acquisition accessory consists of a ring-shaped encapsulated switchable antenna array that can be attached to a conventional colonoscope's tip, as shown in Figure 1. The antenna array comprises two rings of eight antennas, one containing the transmitting and the other the receiving antennas. The antenna elements are cavity-backed slot antennas operating over the 7.6–7.66 GHz range in free space. Figure 2 shows the antenna geometry and S-parameters. The reduced bandwidth is due to the miniaturization of the electrically small antennas, $0.16\lambda \times 0.12\lambda$, as described in a previous paper [23]. The frequency was chosen because the range from 5 GHz to 8 GHz is where there is more contrast in dielectric properties between healthy colon tissue and polyps [27]. In this application, using a high frequency is not a problem since polyp detection does not require penetration into the tissue since they are superficial lesions. The output power of the VNA is −5 dBm, due to the attenuation of the cables and the multiplexer, the power arriving to the antennas is between −13 dBm and −15 dBm. As the antennas have an efficiency of 22%, the radiated power is between 0.007 mW to 0.011 mW at 7.5 GHz. The antenna elements are welded onto a polyamide flexible printed circuit board (PCB) containing microstrip feeding lines and two single-pole-eight-throw (SP8T) radiofrequency switches. This assembly is wrapped around a 3D printed piece that adapts the PCB with the colonoscope. Finally, it is encapsulated with a biocompatible 3D printed resin to protect the PCB from moisture and avoid injuring the colon mucosa tissue. The final dimensions of the accessory are 30 mm in length by 20 mm in diameter, exceeding the colonoscope's diameter by less than 3 mm. The dimensions and shape of the accessory device ensure non-obstruction of the colonoscope's front tip, maintain the maneuverability of the colonoscope, avoid camera concealment, and prevent injuries to the patient. Two slim 500 mm in length and 1.13 mm in diameter coaxial cables transmit the microwave signals, and eight wires transmit the switches' control signals. Miniature connectors are used for a non-bulky final assembly.

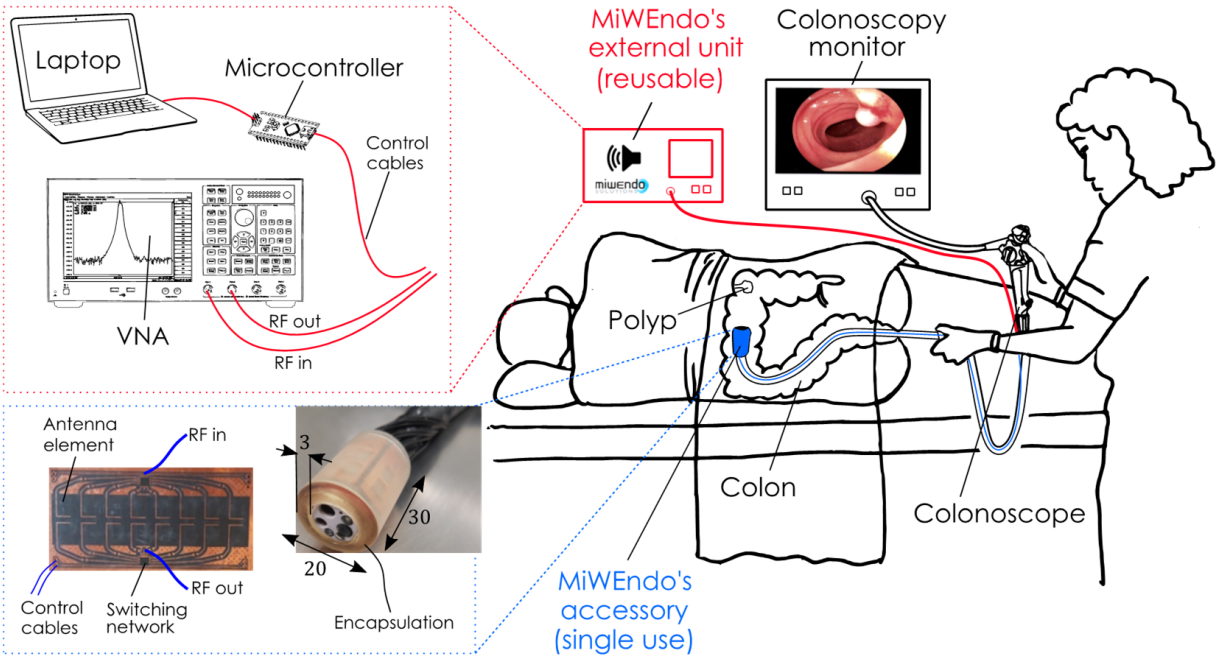

Figure 1. MiWEndo's microwave endoscopy system is composed by an accessory attachable at the distal tip of a standard colonoscope (**bottom left**) and an external processing unit (**top left**). MiWEndo generates an acoustic signal when a polyp is detected to warn the endoscopist during a colonoscopy exploration (**right**). Encapsulation size is in mm.

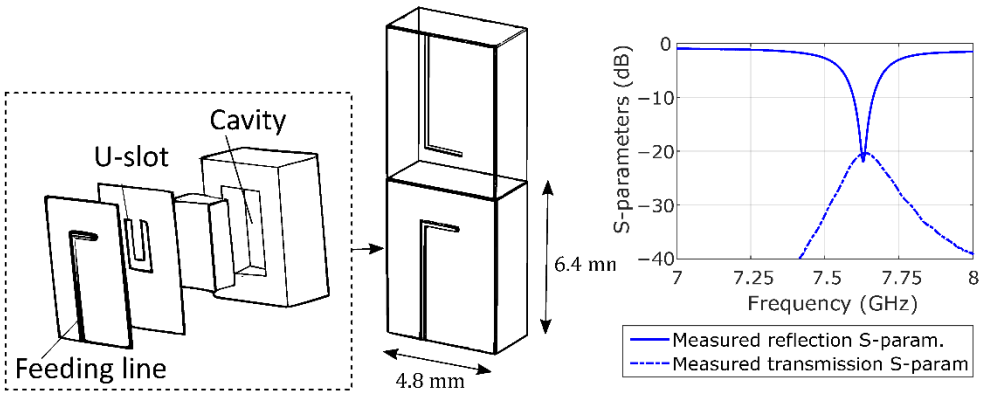

(**a**) (**b**)

Figure 2. (**a**) Schematic of the cavity-backed slot antenna and a transmitting and receiving antenna pair. (**b**) Measured transmission and reflection S-parameters.

2.2. Setup for Ex Vivo Human Colon Measurements

The colon is the last part of the gastrointestinal tract. It has a segmented appearance due to a series of folds, and it is about 1500 mm long and 40–90 mm in diameter. Polyps are slow-growing overgrowths of the colonic mucosa protruding into the lumen.

This study was performed at the Pathology Unit of Hospital Clínic de Barcelona and was conducted according to the guidelines of the Declaration of Helsinki and approved by the Institutional Review Board of Hospital Clínic de Barcelona (protocol code HCB/2017/0519 and date of approval 29 June 2017). Informed consent was obtained from all subjects involved in the study. A total of 15 patients undergoing surgical colectomies were enrolled in the study. The protocol, shown in Figure 3, was defined in close collaboration with the medical staff to reduce the manipulation of the samples and time between excision and measurement. The colon samples were obtained from surgical colectomies performed in an operating room with the shortest possible cold ischemia time and without any conservation treatment (i.e., without formaldehyde) to preserve their physical and dielectric properties. Samples from patients that underwent previous radiation therapy or chemotherapy were excluded. Next, a pathologist opened the colon sample containing a neoplasm longitudinally, placed it in a hermetically sealed plastic container, and transported it to the measurement room. Immediately after sample arrival, we performed the exploration with MiWEndo's accessory. To reproduce a realistic colonoscopy exploration with ex vivo colon fragments, we created a colon fixation setup and a positioning setup to move MiWEndo's accessory along the ex vivo colon lumen shown in Figure 4a. The positioning setup was composed of a T-shaped metallic structure fixed on a plastic base. The metallic structure holds a plastic bar that simulates a colonoscope tube. MiWEndo's accessory was attached at the tip of the plastic bar. The colon sample was fixed around a tube of expanded polystyrene and externally wrapped with a soaker pad. Expanded polystyrene behaves like air for microwaves and therefore has a minimal impact on the radiated electromagnetic fields. It represents a realistic situation since, during a colonoscopy, the colon is expanded using carbon dioxide insufflation to increase colon visualization. The wrapped sample was placed on a platform with L-shaped plastic pieces to fix the sample during the procedure, and the platform was placed on a lifting platform to control the vertical position. Finally, the lifting platform was placed next to the positioning setup. The plastic bar with the MiWEndo's accessory attached at its tip was manually pushed inside the tube of expanded polystyrene that models the colon lumen in steps of 4 mm. A measurement was made before each step until reaching the end of the sample. Table 1 shows the characteristics of the human colon samples measured. Samples 11, 12, and 13 were wrapped around a curved polystyrene foam to model a colon angulation, simulating

a more challenging situation. Moreover, Sample 12 presented a suboptimal cleaning of the colon with some debris along the mucosa.

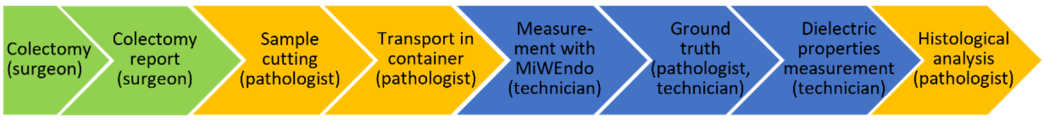

Figure 3. Protocol for the acquisition of electromagnetic measurements within medical routine.

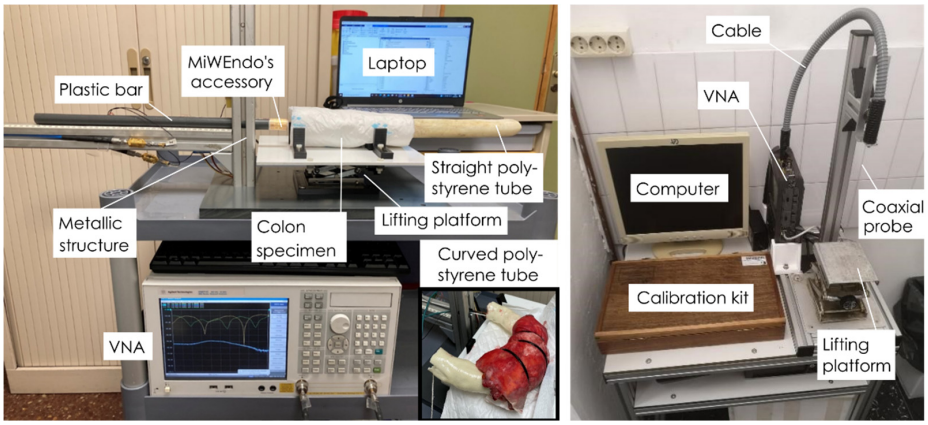

(**a**) (**b**)

Figure 4. Setup for ex vivo human colon measurements: (**a**) setup for the exploration of ex vivo human colon samples with MiWEndo's accessory; (**b**) setup for measuring the dielectric properties of ex vivo colon samples with the open-ended coaxial probe method.

Table 1. Characteristics of the trajectories measured in human colon models and performance evaluation of the implemented algorithm in terms of sensitivity and specificity.

Patient	Age	Type of Neoplasm	Neoplasm Size (mm)	Sample Length (mm)	Sensitivity (%)	Specificity (%)
1	86	Adenoma with HGD [1]	10	200	100	80
2	64	Adenocarcinoma [2]	50	220	100	94.12
3	46	Adenocarcinoma	36	80	100	100
4	37	Adenoma with HGD	32	155	100	87.50
5	83	Adenocarcinoma	48	190	100	90.91
6	60	Adenocarcinoma	37	190	100	77.78
7	57	Adenocarcinoma	65	330	100	88.37
8	68	Adenocarcinoma	15	320	100	85.71
9	86	Adenoma with HGD	23	270	100	86.54
10	85	Adenocarcinoma	34	285	100	87.23
11	45	Adenocarcinoma [3]	32	260	100	83.33
12	75	Adenocarcinoma [4]	35	180	100	86.36
13	91	Adenocarcinoma [3]	40	160	100	84.21
14	62	Adenocarcinoma [3]	37	228	100	92.86
15	81	Adenocarcinoma	63	97	100	100

[1] HGD means high grade dysplasia and refers to precancerous changes in the cells. [2] Adenocarcinoma is a cancer that begins in glandular cells. [3] Curved trajectories emulating a colon fold. [4] Trajectory with a suboptimal colon cleaning.

After exploring the colon sample with MiWEndo's accessory, the sample was removed from the measurement setup. With the help of the pathologist the position position of the lesion with respect to the beginning of the trajectory was registered. These data constitute the ground truth necessary to evaluate the algorithm's performance. Next, the dielectric properties of the colon mucosa and the neoplasm were measured using the open-ended coaxial probe method using the N1501A Dielectric Slim Form Probe Kit,

Keysight, Santa Rosa, California, US with the N1500A Materials Measurement Software Suite version 16.0.16092801, Keysight, Santa Rosa, CA, USA connected to a vector network analyzer Keysight E5071C. We performed three measurements on the neoplasm and three measurements on three equidistant locations on the healthy mucosa (start, center, and end). The different tissues were identified by a pathologist prior to the measurement with the coaxial probe. We followed the recommended procedure for obtaining high quality measurements with the open ended coaxial probe [27,28]. The setup is depicted in Figure 4b. The entire protocol was performed between 30 min and one hour after colon resection. Finally, the specimens were sent to the Pathology Department for the histological analysis of the neoplasms.

2.3. Polyp Detection Algorithm for Microwave-Assisted Colonoscopy

The MiWEndo's accessory was moved inside the colon model in a straight trajectory throughout the center of the lumen to simulate a colonoscopy exploration for polyp detection. A microwave image of a cross-section of the colon (XY plane) was obtained for each step in the trajectory, which was performed in 4 mm increments along the z-axis. Figure 5 presents the geometry of the imaging setup. Each step in the trajectory and its microwave image is referred to as a frame, being n the index of the current frame.

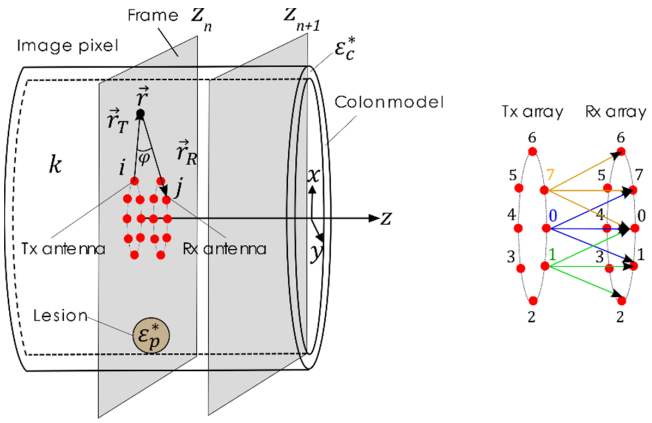

Figure 5. Geometry of the imaging problem: (**a**) schematic of the ex vivo colon model with a lesion of complex permittivity $\varepsilon_p{}^*$ and the acquisition array moving along the z-direction in the colon lumen. (**b**) Transmitting and receiving array configuration, e.g., for the transmitter $i = 0$, a measurement is taken with the 3 closest receiving antennas, $j = 7,\ 0,\ 1$ depicted in blue, for the transmitter $i = 1$ a measurement is taken with antennas $j = 0,\ 1,\ 2$ depicted in green, for the transmitter $i = 7$ a measurement is taken with the antennas, $j = 6,\ 7,\ 0$ in orange.

The data for creating the microwave image at each frame is obtained by subsequently illuminating the colon tissue with a microwave signal radiating from a transmitting antenna and measuring the total field at the three receiving antennas that are closest to the transmitting one (the adjacent antenna and the two diagonal antennas). The measured total field results from the interaction of the incident microwaves and the colon tissues and therefore contains information about the spatial distribution of the dielectric properties of the colon. The process is repeated for each of the 8 transmitting antennas to scan the entire perimeter of the colon. In total, 24 combinations of transmission S-parameters are measured and used to produce the microwave image the frame's cross-sectional slice of the colon.

The microwave image reconstructions were obtained at a single frequency of 7.6 GHz corresponding to the center frequency of the antennas. Since the antennas are narrowband, using more frequencies within their bandwidth does not provide additional independent information for reconstruction.

A three-step algorithm is used to obtain the output, i.e., the acoustic signal when a polyp is detected, for each measured frame n.

2.3.1. Calibration

The aim of the calibration step is to clean the total field of unwanted effects including: the unknown distance to the colon walls, the colon folds, the angulations, etc., and to keep the response due to the presence of the polyp. To fulfill this purpose, a calibration strategy, which was given the name of automatic temporal (AT) subtraction calibration, was implemented [26]. The AT subtraction calibration relies on the hypothesis that the impact on the scattered field that is caused by a polyp is much more important than the one produced by any other of the previously mentioned effects. Hence, for each frame, this strategy identifies, from the pool of previous frames, the frame with the most similar scattered field and subtracts it. By doing so, the only effect that would remain after the calibration is the polyp response, while the rest of undesirable effects would be minimized since they have a similar effect on the subtracted frames. The similarity between frames is computed using the modified Hausdorff distance, whose potential as S-parameters similarity measurer has already been proven [29]. Therefore, the frame with the most similar S-parameters to the current one is computed as follows:

$$S' : \max\left(\| S(n) - S' \|\right)) = \min\left(\max\left(\| S(n) - S'_i \|\right)\right) \; for \; i = 1, \ldots, n-1 \tag{1}$$

where S(n) corresponds to the frame that is being calibrated, S′ to the most similar frame to S(n), and S'_i to the previously acquired frames.

2.3.2. Focuser

Once the data is calibrated, a modified monofocusing algorithm [30] is applied to obtain an image of the dielectric contrast profile $I_{z_n}\left(\vec{r}\right)$:

$$I_{z_n}\left(\vec{r}\right) = \left| \sum_{j=(i-1)_{N_a}}^{(i+1)_{N_a}} \sum_{i=0}^{N_a-1} E_s^2\left(\vec{r}_{T_i}, \vec{r}_{R_j}, z_n\right) J_1^2\left(k\left|\vec{r}_{R_j} - \vec{r}\right|\right) e^{j2(k|\vec{r}_{R_j} - \vec{r}| + \varphi)} \right| \tag{2}$$

where $k = 2\pi c f$ is the wavenumber, φ is the angle between the transmitting and the receiving antennas, and E_s is the scattered electric field. This focuser method provides the image of the dielectric contrast profile. The constant c is the speed of light since the colon is insufflated with carbon dioxide during the procedure.

2.3.3. Detector

The detection method implemented is based on a forecasting exponential smoothing method for the detection of outliers [31,32]. We have observed that high amplitudes in the microwave images usually correspond to the presence of a polyp, but the high amplitude values are not comparable between different trajectories (different colon specimens). Therefore, we can detect the presence of a polyp by finding outlying values of the maximum amplitude of the reconstructed microwave image compared to previous frames in the same trajectory.

The first step in the detection algorithm is to compute an estimate of the maximum amplitude of the image for the next frame, $s(n+1)$, based on the previous estimation of the current frame and its actual maximum amplitude, $y(n)$, as follows:

$$s(n+1) = \alpha \times y(n) + (1-\alpha) \times s(n) \tag{3}$$

where α is a constant between [0, 1]. The next step is to compute the confidence band b, in which the next maximum amplitude of the image will likely lie.

$$b(n+1) = s(n+1) \; \pm \; [\alpha \times [y(n) - s(n)] + (1-\alpha) \times b(n)] \times \delta \tag{4}$$

Here δ is a constant higher than 1. When the maximum reconstructed amplitude of the analyzed frame lies above its confidence band, the algorithm concludes that a polyp is detected and activates the acoustic signal.

3. Results

3.1. Sample Characterization Results

Using the data provided in the pathology report, we identified and labeled all the measured frames: healthy mucosa, adenomas with high grade dysplasia (HGD), and adenocarcinomas. Note that high grade dysplasia refers to precancerous changes in the cells. Table 1 summarizes the main characteristics of the 15 colon examinations, and Figure 6 shows the relative permittivity and conductivity of the healthy colon mucosa and neoplasm of each patient. If we look at the dielectric properties of each patient individually, we see that the dielectric properties of the neoplasm are always higher than those of the healthy mucosa. However, there is considerable variability between patients. This makes it impossible to establish a threshold that allows the differentiation between the healthy mucosa and the neoplasm for all patients. It is worth mentioning that accurately measuring the dielectric properties of healthy mucosa is very difficult since it is a very fine tissue, between 0.5 and 2 mm. Moreover, the part opposite the lumen was covered with very variable amounts of fat. Since we could not manipulate the samples so as not to alter the subsequent pathological analysis, the uniformity of the samples cannot be guaranteed. So, part of the variability between patients could be attributed to this issue.

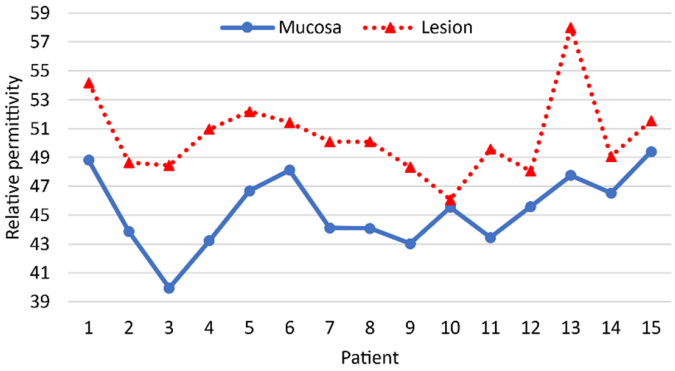

(**a**)

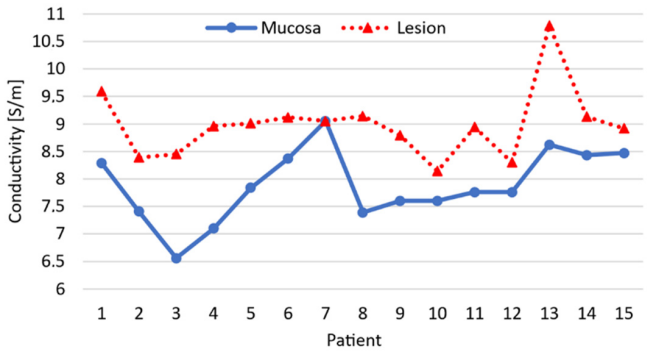

(**b**)

Figure 6. Dielectric properties of the healthy colon mucosa and the neoplasm at 7.6 GHz for each patient was measured with an open-ended coaxial probe. (**a**) Relative permittivity, (**b**) conductivity.

3.2. Polyp Detection Results

Following data acquisition and processing, the results of the microwave-based colonoscopy were obtained. The performance of the method to detect polyps in a trajectory is evaluated using the sensitivity and specificity. The sensitivity, also called the true positive (TP) rate, measures the percentage of cases having a polyp that are correctly diagnosed as having the

lesion. A false negative (FN) occurs when a negative result is reported to a trajectory that does have a polyp. The specificity, also called the true negative (TN) rate, measures the percentage of healthy cases that are correctly identified as not having any polyp. A false positive (FP) is reported when the test wrongly indicates that a polyp is present. The values of sensitivity and specificity are related to TP, FP, TN, and FN values as follows:

$$\text{Sensitivity } (\%) = \frac{\text{TP}}{\text{TP} + \text{FN}}, \qquad \text{Specificity } (\%) = \frac{\text{TN}}{\text{TN} + \text{FP}} \tag{5}$$

Table 1 shows that in all the 15 cases the neoplasm has been detected with microwave-based colonoscopy. The overall sensitivity is 100% and the specificity is 87.43%.

As an example, Figure 7a shows the evolution of the normalized maximum amplitude of the reconstructed image registered in each step of the trajectory, where it is possible to appreciate the increase of amplitude due to the presence of the lesion. The reconstructed image has been obtained using Equation (2). Figure 7c presents the normalized maximum amplitude of the microwave image in front of each pair of antennas, and, here, it is moreover possible to observe that the impact of the lesion is much more significant on the antennas 0–7, 0, 1 (Transmitter 0 and Receivers 7, 0, and 1), which are the ones that face the neoplasm. Overall, both figures demonstrate that the presence of the lesion produce an increase in the amplitude of the reconstructed images, which is not registered in the healthy tissue.

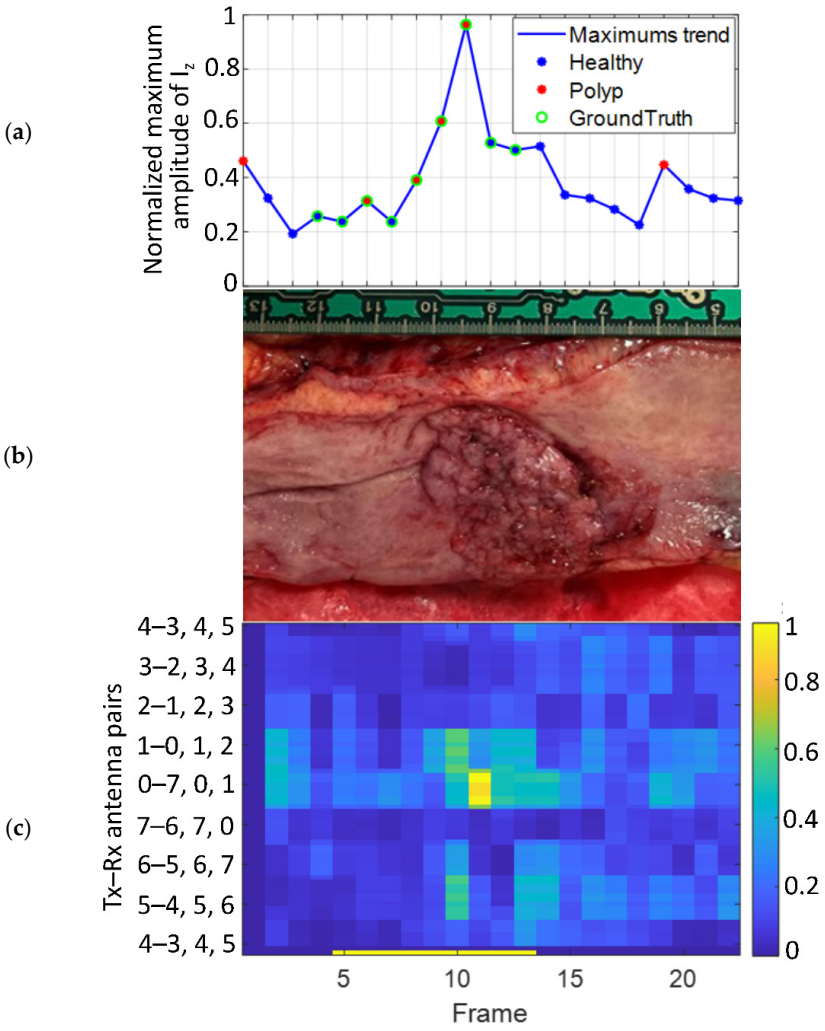

Figure 7. Results of Patient 4. (**a**) The evolution of the normalized maximum amplitude of the reconstructed image for each frame of the trajectory, (**b**) photograph of the colon sample with an adenoma with HGD, (**c**) normalized maximum amplitude in front of all the antenna combinations.

4. Discussion

Missed lesions at colonoscopy are as high as 22% and have important clinical consequences. In the last years, many efforts have been made to improve the performance of endoscopy, but the common limitation of these methods is that they cannot detect what is not displayed by the camera.

In this study we have shown that the improved version of the algorithm is able to detect neoplastic lesions in human colon models. To do so, the MiWEndo microwave colonoscopy accessory device attached to a colonoscopy simulating setup was used. The system can detect neoplastic lesions on the full perimeter of the colon based on the changes in their dielectric properties and may be used to complement the endoscopic image. The system has been designed to be compatible with colonoscopy, ensure a full coverage and produce minimal changes to the current clinical practice. The final dimensions of the acquisition accessory device are 30 mm in length by 20 mm in diameter, with a total thickness of 3 mm. The dimensions and shape of the device ensure non-obstruction of the front tip of the colonoscope, avoiding injuring the patient or hindering the maneuverability of the colonoscope. The antennas work at 7.6 GHz over a narrow bandwidth and with an acceptable coupling.

A frequency domain imaging reconstruction algorithm based on Fourier backprojection preceded with an automatic temporal subtraction calibration that has been developed to obtain cross sectional images of the colon. An automatic detection step based on exponential smoothing was applied to obtain an output easy to interpret by the physicians, i.e., and acoustic alarm, when a polyp is detected. This kind of output was inspired by the acoustic parking system for automobiles. The system provides an audible warning with a series of beeps as the car, or the endoscope, moves nearer a stationary object, or a polyp. The algorithm is fast and able to work in real time, delivering around 10 frames/s. In terms of performance, the algorithm has reached a sensitivity of 100% and a specificity of 87.43%. No significant degradation of performance has been observed when the trajectory is not straight (trajectories 11, 13, and 14). This may indicate that the algorithm, and especially the calibration, can deal with the angulations of the colon. Debris in the colon (trajectory 12) did not degraded performance either. In the absence of further validation and to confirm this in future tests, it could be examined as to whether microwave-assisted colonoscopy could reduce the need for colon preparation. The impact of poor preparation is important since it forces to repeat the colonoscopy. In addition, the preparation required for the patient to clean the colon is the most uncomfortable part of the colonoscopy, according to patients. It is worth mentioning that by changing the value of the constants α and δ used in the exponential smoothing method it is possible to tune the sensitivity and specificity values. We decided to force an optimal sensitivity because our device is aimed to prevent polyps from being missed once combined with colonoscopy. A suboptimal sensitivity can be accepted because our device is used in conjunction with the colonoscope. In cases where the acoustic signal is heard, the finding will always be confirmed with the video from the colonoscope.

Regarding the dielectric and pathologic characterization of the lesions, at 7.6 GHz healthy colon mucosa and neoplastic lesions exhibit inter-patient contrast in dielectric properties that allow its differentiation. However, the variation between patients do not allow to fix a permittivity threshold to differentiate all the healthy and neoplastic tissues. This is not a problem for the MiWEndo's system since the detection criteria is defined for each patient.

The main limitation of this study is the low number of adenomas studied. The device was validated in ex vivo human colons that usually are surgically resected because they have already developed cancer. These lesions are commonly big and are not representative of what is commonly found in a regular colonoscopy. The second limitation is that the real-time acquisition system has not been tested. In this study, a measurement was taken after each trajectory step manually. To make the acquisition in real time, a second generation of external unit is being developed. The last limitation is that the device was not attached

at the end of a real endoscope and the maneuverability and safety could not be assessed. Safety must be guaranteed on two fronts: energy safety and mechanical safety. In terms of energy, we refer to limit the radiation to avoid any biological effect to the patient's mucosa, i.e., heating, but also ensure the electrical safety and electromagnetic compatibility. In terms of mechanical safety, the accessory device must be designed with smooth surface, using biocompatible materials in the parts that are in contact with the patient and the materials must be clean, i.e., with low bioburden.

For all these reasons, we are developing increasingly realistic anatomic models with folds and polyps of different sizes and shapes made of materials that mimic the dielectric properties of colon tissues. In the phantoms we also can study different trajectories, varying the distance between the antennas and the colon wall while controlling the ground truth, i.e., the position of the polyp. The results with the simplest phantom can be found in [24]. We are also planning new studies in animal models to check the maneuverability and the inter-compatibility with other endoscopic devices used in real explorations such as forceps or electrocautery tools.

5. Conclusions

This paper presents the algorithm validation of a microwave colonoscopy system with 15 ex vivo human colons with neoplastic lesions. The system consists of an acquisition accessory attachable to the distal tip of a standard colonoscope connected to an external processing unit. The algorithm is composed of three steps: calibration, focusing, and automatic detection. A sensitivity of 100% and a specificity of 87.43% was achieved, indicating that the detection algorithm is able to deal with real human colon tissues. The algorithm was able to deal with colon angulations. This confirmed what we observed with phantoms, where a more realistic movement within the colon was reproduced. This demonstrates that the calibration method can deal with the changing distances between the antennas and the colon wall. In one trajectory, the algorithm was able to detect the lesion even in suboptimal cleaning conditions.

We are currently carrying out a measurement campaign with a new phantom extracted from a 3D model of a real patient with angulations and folds. With this model, several trajectories will be measured with the accessory attached to a real colonoscope and the algorithm will be used in real time. This setup will allow the conclusion of the algorithm validation with more challenging conditions before starting the clinical phase.

Author Contributions: Conceptualization, M.G. and G.F.-E.; methodology, M.G.; software, W.D., A.G. and L.M.N.; validation, M.G., R.S. and S.M.; formal analysis, M.G., W.D. and A.G.; investigation, M.G., W.D., A.G. and L.M.N.; resources, M.G. and G.F.-E.; data curation, W.D. and A.G.; writing—original draft preparation, M.G.; writing—review and editing, M.G. and W.D.; visualization, G.F.-E.; supervision, M.G.; project administration, I.B.; funding acquisition, I.B. All authors have read and agreed to the published version of the manuscript.

Funding: This research was funded by the European Union's Horizon 2020 Research and Innovation Programme, grant number 960251, and by the Spanish Ministry of Science and Innovation, grant number DIN2019-010857/AEI/10.13039/501100011033.

Institutional Review Board Statement: The study was conducted according to the guidelines of the Declaration of Helsinki and approved by the Institutional Review Board of Hospital Clínic de Barcelona (protocol code HCB/2017/0519 and date of approval 29 June 2017).

Informed Consent Statement: Written informed consent was obtained from the patient(s) to publish this paper.

Data Availability Statement: All data generated or analyzed during this study are included in this article. Further enquiries can be directed to the corresponding author.

Acknowledgments: The authors acknowledge the infrastructure and support of the Pathology Unit of Hospital Clínic de Barcelona and especially to Miriam Cuatrecasas and Sandra López-Prades, who helped us in the sample collection, manipulation, and lesion identification. The authors also want to

thank the Universitat Politècnica de Catalunya for letting us have the coaxial probe and especially to Joan O'Callaghan for his advice.

Conflicts of Interest: M.G., I.B., and G.F.-E. are shareholders of MiWEndo Solutions. W.D., R.S., A.G., S.M. and L.M.N. declare no conflict of interest.

References

1. Ferlay, J.; Ervik, M.; Lam, F.; Colombet, M.; Mery, L.; Piñeros, M. Global Cancer Observatory: Cancer Today. *Int. Agency Res. Cancer* **2018**, *3*, 2019.
2. Bray, F.; Ferlay, J.; Soerjomataram, I.; Siegel, R.L.; Torre, L.A.; Jemal, A. Global cancer statistics 2018: GLOBOCAN estimates of incidence and mortality worldwide for 36 cancers in 185 countries. *CA Cancer J. Clin.* **2018**, *68*, 394–424. [CrossRef]
3. Surveillance Research Program, National Cancer Institute SEER*Stat Software. Available online: Seer.cancer.gov/seerstat (accessed on 8 October 2021).
4. Müller, A.D.; Sonnenberg, A. Prevention of colorectal cancer by flexible endoscopy and polypectomy. A case-control study of 32,702 veterans. *Ann. Intern. Med.* **1995**, *123*, 904–910. Available online: http://www.ncbi.nlm.nih.gov/pubmed/7486484 (accessed on 12 May 2017). [CrossRef]
5. Winawer, S.J.; Zauber, A.G.; Ho, M.N.; O'Brien, M.J.; Gottlieb, L.S.; Sternberg, S.S.; Jerome, D.W.; Melvin, S.; John, H.B.; Joel, F.P.; et al. Prevention of Colorectal Cancer by Colonoscopic Polypectomy. *N. Engl. J. Med.* **1993**, *329*, 1977–1981. Available online: http://www.ncbi.nlm.nih.gov/pubmed/8247072 (accessed on 12 May 2017). [CrossRef]
6. van Rijn, J.C.; Reitsma, J.B.; Stoker, J.; Bossuyt, P.M.; van Deventer, S.J.; Dekker, E. Polyp miss rate determined by tandem colonoscopy: A systematic review. *Am. J. Gastroenterol.* **2006**, *101*, 343–350. [CrossRef]
7. Samadder, N.J.; Curtin, K.; Tuohy, T.M.; Pappas, L.; Boucher, K.; Provenzale, D.; Rowe, K.G.; Mineau, G.P.; Smith, K.; Pimentel, R.; et al. Characteristics of missed or interval colorectal cancer and patient survival: A population-based study. *Gastroenterology.* **2014**, *146*, 950–960. [CrossRef]
8. Lee, T.; Rees, C.; Blanks, R.; Moss, S.; Nickerson, C.; Wright, K.; James, P.W.; McNally, R.J.Q.; Patnick, J. Colonoscopic factors associated with adenoma detection in a national colorectal cancer screening program. *Endoscopy* **2014**, *46*, 203–211. Available online: http://www.ncbi.nlm.nih.gov/pubmed/24473907 (accessed on 12 May 2017). [CrossRef]
9. East, J.E.; Saunders, B.P.; Burling, D.; Boone, D.; Halligan, S.; Taylor, S.A. Surface visualization at CT colonography simulated colonoscopy: Effect of varying field of view and retrograde view. *Am. J. Gastroenterol.* **2007**, *102*, 2529–2535. [CrossRef]
10. Corley, A.C.; Jensen, C.D.; Marks, A.R.; Zhao, W.K.; Lee, J.K.; Doubeni, C.A.; Zauber, A.G.; de Boer, J.; Fireman, B.H.; Schottinger, J.E.; et al. Adenoma Detection Rate and Risk of Colorectal Cancer and Death. *N. Engl. J. Med.* **2014**, *370*, 1298–1306. [CrossRef]
11. Ngu, W.S.; Bevan, R.; Tsiamoulos, Z.P.; Bassett, P.; Hoare, Z.; Rutter, M.D.; Clifford, G.; Totton, N.; Lee, T.J.; Ramadas, A.; et al. Improved adenoma detection with Endocuff Vision: The ADENOMA randomised controlled trial. *Gut* **2019**, *68*, 280–288. [CrossRef]
12. Dik, V.K.; Gralnek, I.M.; Segol, O.; Suissa, A.; Belderbos, T.D.G.; Moons, L.M.G.; Segev, M.; Domanov, S.; Rex, D.K.; Siersema, P.D. Multicenter, randomized, tandem evaluation of EndoRings colonoscopy—Results of the CLEVER study. *Endoscopy* **2015**, *47*, 1151–1158. [CrossRef]
13. Ngu, W.S.; Rees, C. Can technology increase adenoma detection rate? *Ther. Adv. Gastroenterol.* **2018**, *11*, 1–18. [CrossRef]
14. Ahmad, O.F.; Soares, A.S.; Mazomenos, E.; Brandao, P.; Vega, R.; Seward, E.; Stoyanov, P.D.; Chand, M.; Lovat, L.B. Artificial intelligence and computer-aided diagnosis in colonoscopy: Current evidence and future directions. *Lancet Gastroenterol. Hepatol.* **2019**, *4*, 71–80. Available online: http://www.ncbi.nlm.nih.gov/pubmed/30527583 (accessed on 14 December 2018). [CrossRef]
15. Repici, A.; Badalamenti, M.; Maselli, R.; Correale, L.; Radaelli, F.; Rondonotti, E.; Ferrara, E.; Spadaccini, M.; Alkandari, A.; Fugazza, A. Efficacy of Real-Time Computer-Aided Detection of Colorectal Neoplasia in a Randomized Trial. *Gastroenterology* **2020**, *159*, 512–520. [CrossRef]
16. Kumashiro, R.; Konishi, K.; Chiba, T.; Akahoshi, T.; Nakamura, S.; Murata, M.; Tomikawa, M.; Matsumoto, T.; Maehara, Y.; Hashizume, M. Integrated endoscopic system based on optical imaging and hyperspectral data analysis for colorectal cancer detection. *Anticancer Res.* **2016**, *36*, 3925–3932. Available online: https://ar.iiarjournals.org/content/36/8/3925 (accessed on 10 October 2021).
17. Nikolova, N.K. *Introduction to Microwave Imaging*; Cambridge University Press: Cambridge, UK, 2017; p. 366. Available online: http://ebooks.cambridge.org/ref/id/CBO9781316084267 (accessed on 24 October 2017).
18. Shere, M.; Lyburn, I.; Sidebottom, R.; Massey, H.; Gillett, C.; Jones, L. MARIA® M5: A multicentre clinical study to evaluate the ability of the Micrima radio-wave radar breast imaging system (MARIA®) to detect lesions in the symptomatic breast. *Eur. J. Radiol.* **2019**, *116*, 61–67. Available online: https://www.sciencedirect.com/science/article/pii/S0720048X19301512?via%3Dihub (accessed on 26 March 2020). [CrossRef]
19. O'Loughlin, D.; O'Halloran, M.; Moloney, B.M.; Glavin, M.; Jones, E.; Elahi, M.A. Microwave breast imaging: Clinical advances and remaining challenges. *IEEE Trans. Biomed. Eng.* **2018**, *65*, 2580–2590. [CrossRef]

20. Toaha Mobashsher, A.; Abbosh, A.M. On-site Rapid Diagnosis of Intracranial Hematoma using Portable Multi-slice Microwave Imaging System. *Auto Moto Patras.Gr* **2016**, *6*, 1–17. Available online: https://www.nature.com/articles/srep37620.pdf (accessed on 8 December 2021). [CrossRef]
21. Meaney, P.M.; Goodwin, D.; Golnabi, A.H.; Zhou, T.; Pallone, M.; Geimer, S.D.; Burke, G.; Paulsen, K.D. Clinical microwave tomographic imaging of the calcaneus: A first-in-human case study of two subjects. *IEEE Trans. Biomed. Eng.* **2012**, *59*, 3304–3313. Available online: http://www.ncbi.nlm.nih.gov/pubmed/22829363 (accessed on 24 October 2017). [CrossRef]
22. Semenov, S.Y.; Posukh, V.G.; Bulyshev, A.E.; Williams, T.C.; Sizov, Y.E.; Repin, P.N.; Souvorov, A.; Nazarov, A. Microwave Tomographic Imaging of the Heart in Intact Swine. *J. Electromagn. Waves Appl. J. Electromagn. Waves Appl.* **2006**, *207*, 873–890. Available online: http://www.tandfonline.com/action/journalInformation?journalCode=tewa20 (accessed on 24 October 2017). [CrossRef]
23. Guardiola, M.; Djafri, K.; Challal, M.; Gonzalez Ballester, M.A.; Fernandez-Esparrach, G.; Camara, O.; Romeu, J. Design and evaluation of an antenna applicator for a microwave colonoscopy system. *IEEE Trans. Antennas Propag.* **2019**, *67*, 4968–4977. [CrossRef]
24. Garrido, A.; Sont, R.; Dghoughi, W.; Marcoval, S.; Romeu, J.; Fernández-Esparrach, G.; Belda, I.; Guardiola, M. Polyp Automatic Detection using Microwave Endoscopy for Colorectal Cancer Prevention and Early Detection. Phantom Validation. *IEEE Access* **2021**, *9*, 148048–148059. [CrossRef]
25. Fernández-Esparrach, G.; Garrido, A.; Sont, R.; Dghoughi, W.; Marcoval, S.; Cuatrecasas, M.; López-Prades, S.; de Lacy, F.B.; Pellisé, M.; Belda, I.; et al. Microwave-Based Colonoscopy: Preclinical Evaluation in an Ex Vivo Human Colon Model. *Gastroenterol. Res. Pract.* **2022**, *2022*, 9522737. [CrossRef]
26. Garrido-atienza, A.; Dghoughi, W.; Robert, J.R.; Garcia, M.G. Preliminary phantom-based dynamic calibration techniques assessment for microwave colonoscopy systems. In Proceedings of the 2022 16th European Conference on Antennas and Propagation (EuCAP), Madrid, Spain, 27 March 2022–1 April 2022; pp. 6–9.
27. Guardiola, M.; Buitrago, S.; Fernández-Esparrach, G.; O'Callaghan, J.M.; Romeu, J.; Cuatrecasas, M.; Córdova, H.; Ballester, M.Á.G.; Camara, O. Dielectric properties of colon polyps, cancer, and normal mucosa: Ex vivo measurements from 0.5 to 20 GHz. *Med. Phys.* **2018**, *45*, 3768–3782. [CrossRef]
28. La Gioia, A.; Porter, E.; Merunka, I.; Shahzad, A.; Salahuddin, S.; Jones, M.; O'Halloran, M. Open-Ended Coaxial Probe Technique for Dielectric Measurement of Biological Tissues: Challenges and Common Practices. *Diagnostics* **2018**, *8*, 40. [CrossRef]
29. Shlepnev, Y. Evaluation of S-Parameters Similarity with Modified Hausdorff Distance. In Proceedings of the 30th IEEE Conference on Electrical Performance of Electronic Packaging and Systems, Austin, TX, USA, 17 October 2021.
30. Zamani, A.; Abbosh, A. Hybrid Clutter Rejection Technique for Improved Microwave Head Imaging. *IEEE Trans. Antennas Propag.* **2015**, *63*, 4921–4931. [CrossRef]
31. Brutlag, J.D. Aberrant behavior detection in time series for network monitoring. In Proceedings of the 14th Systems Administration Conference (LISA 2000), New Orleans, LA, USA, 3–8 December 2000; pp. 139–146.
32. Ward, A.; Glynn, P.; Richardson, K. Internet service performance failure detection. *Perform. Eval. Rev.* **1998**, *26*, 38–43. [CrossRef]

Hindawi
Gastroenterology Research and Practice
Volume 2022, Article ID 9522737, 5 pages
https://doi.org/10.1155/2022/9522737

Research Article

Microwave-Based Colonoscopy: Preclinical Evaluation in an Ex Vivo Human Colon Model

Glòria Fernández-Esparrach,[1,2] **Alejandra Garrido**,[2] **Roberto Sont**,[2] **Walid Dghoughi**,[2] **Sergi Marcoval**,[2] **Miriam Cuatrecasas**,[3] **Sandra López-Prades**,[3] **F. Borja de Lacy**,[4] **María Pellisé**,[1] **Ignasi Belda**,[2] **and Marta Guardiola**[2]

[1]*Endoscopy Unit, Gastroenterology Department, Hospital Clínic, University of Barcelona, CIBEREHD IDIBAPS, Barcelona, Spain*
[2]*MiWEndo Solutions, Barcelona, Spain*
[3]*Pathology Department, Hospital Clínic, University of Barcelona, CIBEREHD, IDIBAPS, Spain*
[4]*Gastrointestinal Surgery Department, Hospital Clinic, University of Barcelona, Spain*

Correspondence should be addressed to Glòria Fernández-Esparrach; mgfernan@clinic.cat

Received 13 October 2021; Accepted 7 January 2022; Published 28 January 2022

Academic Editor: Vincenzo Pilone

Copyright © 2022 Glòria Fernández-Esparrach et al. This is an open access article distributed under the Creative Commons Attribution License, which permits unrestricted use, distribution, and reproduction in any medium, provided the original work is properly cited.

Introduction. Microwave imaging can obtain 360° anatomical and functional images of the colon representing the existing contrast in dielectric properties between different tissues. Microwaves are safe (nonionizing) and have the potential of reducing the visualization problems of conventional colonoscopy. This study assessed the efficacy of a microwave-based colonoscopy device to detect neoplastic lesions in an ex vivo human colon model. *Methods.* Fresh surgically excised colorectal specimens containing cancer or polyps were fixed to a 3D positioning system, and the accessory device was introduced horizontally inside the ex vivo colon lumen and moved along it simulating a real colonoscopy exploration. Measurements of the colon were taken every 4 mm with the microwave-based colonoscopy device and processed with a microwave imaging algorithm. *Results.* 14 ex vivo human colorectal specimens with carcinomas ($n = 11$) or adenomas with high grade dysplasia ($n = 3$) were examined with a microwave-based device. Using a detection threshold of 2.79 for the dielectric property contrast, all lesions were detected without false positives or false negatives. *Conclusions.* This study demonstrates the use of a microwave-based device to be used as an accessory of a standard colonoscope to detect neoplastic lesions in surgically excised colorectal specimens.

1. Introduction

To date, colonoscopy is the most effective diagnostic and therapeutic technique for the prevention of colorectal cancer (CRC), since it allows the identification and removal of polyps with a relatively good accuracy. Several prospective studies demonstrate that colonoscopy with polypectomy reduces the incidence of CRC by 40–90% [1, 2].

Nevertheless, colonoscopy is far from being perfect: 22% of polyps are not detected [3], and the risk of cancer after a negative colonoscopy is still 7.9% [4]. The main cause of this lack of efficacy is the visualization limitation [5] of the optical camera placed at the tip of the endoscope. Studies indicate that 13.4% of the colon surface area might not be visualized during a standard colonoscopy [6] due to reduced field of vision (<180°), inhomogeneous illumination, colon angulation and folds, and poor cleaning. In recent years, several devices and technologies have been developed to improve the detection rate of polyps, such as high-definition endoscopes, endoscopes with multiple lenses (retrovision capability), and mucosal flattening accessories [7].

Microwave imaging can obtain anatomical and functional images of the interior of the human body representing the existing contrast in dielectric properties between different tissues. Microwaves can generate images without restriction of the field of view (360°), are safe (nonionizing and without thermal effect), and offer a fair trade-off between resolution and light opaque tissue penetration [8, 9],

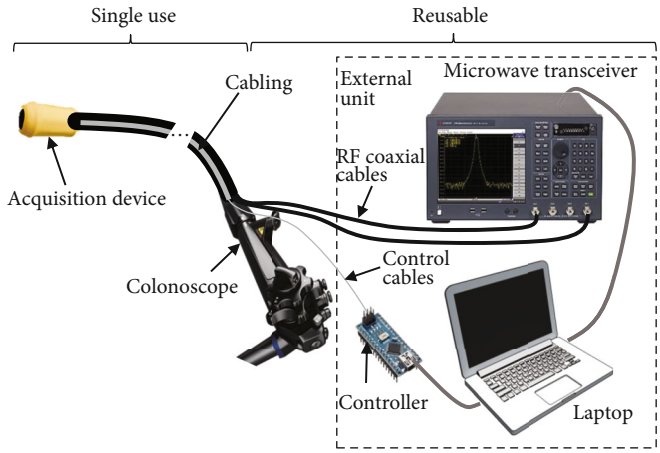

Figure 1: The imaging system consists of a cylindrical ring-shaped acquisition device attached to the tip of a colonoscope connected via cables to the external unit. The external unit consists of a microwave transceiver, a microcontroller, and a laptop.

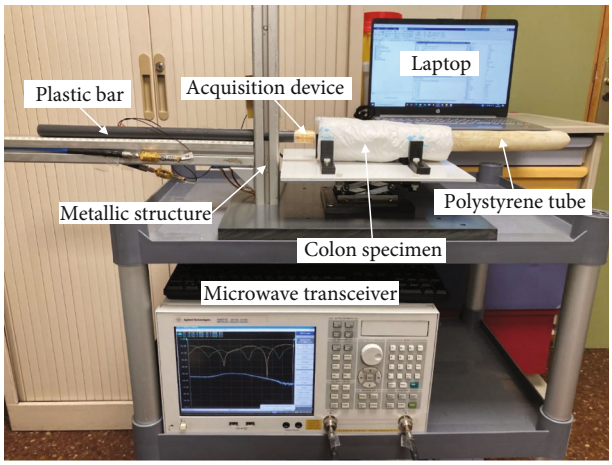

Figure 2: Measurement setup. The colon is wrapped around a polystyrene tube, and the acquisition device is attached to the tip of a plastic bar and connected to the microwave transceiver, the microcontroller, and the laptop.

therefore, potentially reducing visualization problems of conventional colonoscopy. We recently demonstrated that the dielectric properties correlate with the malignancy and grade of dysplasia of colorectal polyps [10]. For these reasons, microwave imaging has the potential to complement conventional colonoscopy to improve both polyp detection rate and in situ tissue classification.

This study assessed the potential of microwave-based colonoscopy to detect neoplastic lesions in an ex vivo human colorectal model.

2. Materials and Methods

2.1. Microwave-Based Accessory Device Description. The imaging system consists of (1) a cylindrical ring-shaped acquisition device that can be attached to the tip of a conventional colonoscope; and (2) an external unit with a microwave transceiver, a controlling unit, and a laptop as a processing unit. The acquisition device contains two switched arrays of eight antennas organized in two rings, one containing the transmitters and the other the receivers [11] that are encapsulated and are connected via cables to the external unit (Figure 1). The dimensions of the acquisition device are 30 mm in length by 20 mm in diameter, having a total thickness of 2.5 mm. The dimensions and shape of the device ensure nonobstruction of the front tip of the colonoscope, avoiding camera concealment, injuring the patient or hindering the maneuverability of the colonoscope.

2.2. Microwave-Based Colonoscopy Setup for Ex Vivo Colon Measurements. To be able to reproduce a real colonoscopy exploration, a 3D positioning system was built (Figure 2) as described elsewhere [12]. The measurement setup is composed by an L-shaped metallic structure fixed on a plastic base. The metallic structure holds a plastic bar that simulates a colonoscope, and the acquisition device is attached at the tip. With this bar, the accessory device was introduced horizontally inside the ex vivo colon or rectal lumen and was moved along it to obtain the measurements.

Surgically excised colorectal specimens containing cancer or polyps were used for the measurements. Immediately after the excision, the fresh specimens were opened longitudinally and then fixed around a tube made of expanded polystyrene and wrapped with a soaker pad. Expanded polystyrene behaves like air for microwaves and therefore does not interfere with measurements. After the procedure, the specimens were sent to the Pathology Department for tissue processing and histological analysis. The protocol was approved by the Ethics Committee of Hospital Clinic of Barcelona, and patients gave written informed consent.

2.3. Microwave Imaging Method for Colonoscopy Description. Microwave imaging is based on illuminating the colon with a microwave signal emanating from one transmitting antenna. The total received field, resulting from the interaction of the incident microwaves, and the colorectal tissues are then measured at the receiving antenna adjacent to the active transmitting antenna. The previous process is repeated for each transmitting antenna located around the tip of the

Table 1: Histology type and size of the lesions.

Patient	Age	Histology type of the lesion	Size (mm)
1	86	Adenoma with HGD	10
2	64	Adenocarcinoma	50
3	46	Adenocarcinoma	36
4	37	Adenoma with HGD	32
5	83	Adenocarcinoma	48
6	60	Adenocarcinoma	37
7	57	Adenocarcinoma	65
8	68	Adenocarcinoma	15
9	86	Adenoma with HGD	23
10	85	Adenocarcinoma	34
11	45	Adenocarcinoma	32
12	91	Adenocarcinoma	40
13	62	Adenocarcinoma	37
14	81	Adenocarcinoma	63

HGD: high grade dysplasia.

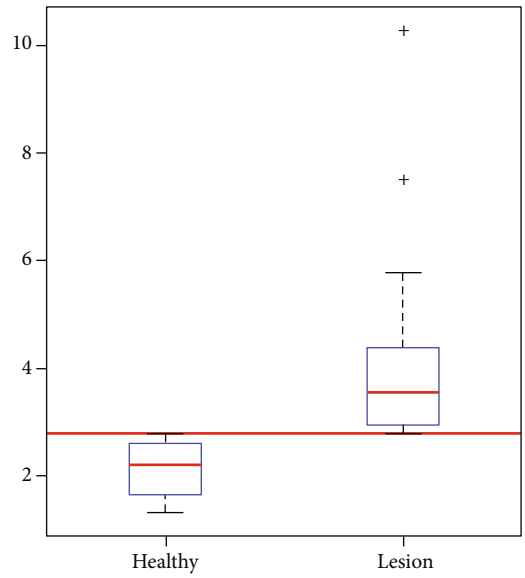

Figure 3: Reconstructed maximum dielectric property contrast of each patient and frame obtained with microwave-based colonoscopy for healthy mucosa areas and for lesions. The detection threshold fixed to 2.79 is represented as a horizontal red line. All values above the line are classified as lesion and below as healthy mucosa.

colonoscope, in this way, information is obtained from the entire perimeter of the colon or rectum. The received field contains information of the spatial changes of the dielectric properties of the tissues. By processing the total field with an imaging algorithm, the dielectric property contrast of the colorectal tissues can be retrieved. The information obtained represents a cross-sectional slice of the colon or rectum, which we call a frame. As the colonoscope moves, the acquisition device is continuously scanning frames, thus, covering all colorectal lumen surface.

3. Results

Fourteen colorectal surgical specimens containing carcinomas ($n = 11$) or adenomas with high grade dysplasia ($n = 3$) were examined (Table 1). The median dielectric property contrast was 3.56 (range, 2.79-10.28) for neoplastic lesions and 2.20 (range 1.31-2.78) for normal mucosa. Setting the dielectric contrast threshold at 2.79, all lesions were detected without false positives or false negatives (Figure 3).

The results of the microwave-based colonoscopy can also be represented as an image (Figure 4). The evolution of the measurements in each frame and the correspondence with the location of the lesion are shown in Figure 5.

4. Discussion

In this study, we have demonstrated for the first time the feasibility of using microwaves for diagnosing colorectal neoplasms. To do so, an accessory device attachable at the distal end of a conventional colonoscope has been developed and tested on human ex vivo colorectal surgical specimens with neoplasms.

Missing lesions at colonoscopy are as high as 22% and have important clinical consequences. In the last years, many efforts have been made to improve the performance of endoscopy, mainly based on improvements in the image quality and a better inspection of the mucosa. However, all these technologies (virtual chromoendoscopy, devices that flatten the mucosa, endoscope with retrovision capability…) cannot see what is not captured in the image. Contrarily, our microwave-based device can differentiate between healthy mucosa and neoplastic lesions based on the changes in their dielectric properties and complementing the endoscopic image emitting an alarm when the dielectric contrast is higher than a predefined threshold. The potential of microwave-based colonoscopy is especially relevant in small flat adenomas which constitute the majority of missed lesions. In a previous study, we did not find significant differences in dielectric properties due to the shape of the polyps [10].

The system has been designed to be compatible with colonoscopy, ensure a 360° coverage, and produce minimal changes to the current clinical practice. Concerning the size restrictions, the final dimensions of the acquisition device are 30 mm in length by 20 mm in diameter, having a total thickness of 2.5 mm. The dimensions and shape of the device ensure nonobstruction of the front tip of the colonoscope and avoid injuring the patient or hindering the maneuverability of the colonoscope. The device has recently been verified on a colon phantom that simulates a realistic colonoscopy exploration. The phantom models a section of a colon including the haustrum and allows placement of different polyps. The phantom is composed of gelatin-oil-based materials to mimic the dielectric properties of colon healthy mucosa and polyps with high grade dysplasia [12].

We used the IDEAL model to drive this innovation [13–15]. The IDEAL Framework and Recommendations represent a new paradigm for the evaluation of surgical operations, invasive medical devices, and other complex therapeutic interventions.

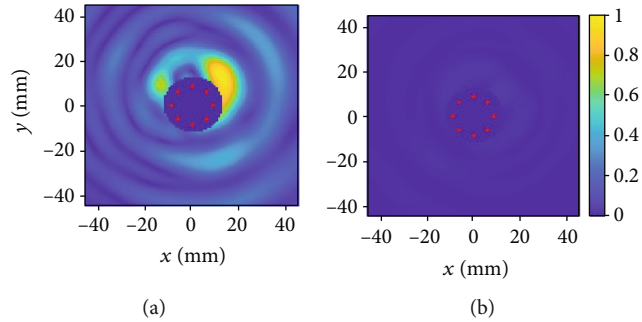

Figure 4: Image frames obtained with microwave-based colonoscopy. The dark blue circle in the middle of the plot indicates the position of the acquisition device, and the red dots the position of each antenna. (a) The highest intensity yellow spot indicates the presence of the polyp. (b) The colors are uniform showing that there are no lesions in the mucosa.

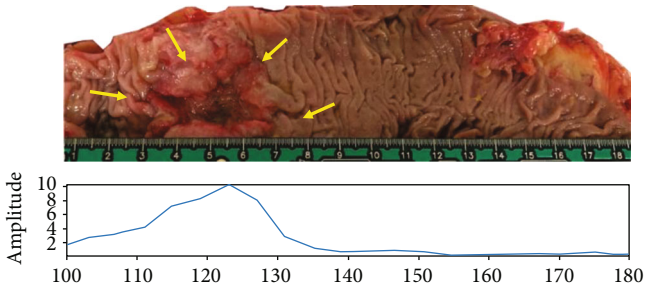

Figure 5: Correlation with the evolution of the maximum amplitude of each successive frame obtained with microwave-based colonoscopy (bottom) and the location of the lesion indicated by the arrows (top). Lower amplitudes around 0.2 are typical of healthy mucosa areas, while neoplastic lesions show high amplitudes close to 1.

The 2009 IDEAL comprised 5 stages: idea (1), development (2a), exploration (2b), assessment (3), and long-term study (4). The original framework was updated in 2019, and a stage 0 was considered, which includes preclinical studies with material testing, simulator, cadavers, animal, and modeling, among others. Preclinical studies are of paramount importance to advance in the conceptualization and preparation before its implementation in patients.

The main limitation of this study is the low number of adenomas studied and reflects the lack of anatomic models provided with haustral folds and polyps made of materials that have the same dielectric properties as the real cases. Therefore, we had to assess our device in ex vivo human colorectal specimens that usually are surgically resected because they have already developed cancer. However, since the grade of dysplasia can be inferred from the dielectric properties as they increase with dysplasia [10], microwave-based colonoscopy has the potential of diagnosing adenomas with low grade dysplasia as well. The second limitation is that measurements were performed in tissues without vascularization. Since the contrast in dielectric properties between different tissues depends on the amount of water, the contrast threshold could be different in an in vivo experiment. The last limitation is that the device was not attached at the end of a real endoscope, and the maneuvrability could not be assessed. We are planning new studies in animal models to check the maneuvrability and intercompatibility with other endoscopic devices, including those that use electrocautery.

In summary, this study demonstrates for the first time the use of a microwave-based device to be used as an accessory of a standard colonoscope to detect neoplastic lesions in surgically excised colorectal specimens.

Data Availability

All data generated or analysed during this study are included in this article. Further enquiries can be directed to the corresponding author.

Conflicts of Interest

Glòria Fernández-Esparrach, Miriam Cuatrecasas, Maria Pellisé, Ignasi Belda, and Marta Guardiola are shareholders of MiWendo Solutions. Alejandra Garrido, Roberto Sont, Walid Dghoughi, Sergi Marcoval, Sandra López-Prades, and F. Borja de Lacy do not have any conflict of interest.

Acknowledgments

This work was supported by the Spanish Ministerio de Economía, Industria y Competitividad, DTS 17/00090 and CERCA Programme/Generalitat de Catalunya. Glòria Fernández Esparrach had a personal grant from Instituto de Salud Carlos III (PI17/00894). Alejandra Garrido acknowledges the financial support from DIN2019-010857/AEI/10.13039/501100011033. Roberto Sont, Marta Guardiola, and Ignasi Belda acknowledge the financial support from the European Union's Horizon 2020 research and innovation programme under grant agreement no. 960251.

References

[1] A. D. Müller and A. Sonnenberg, "Prevention of colorectal cancer by flexible endoscopy and polypectomy. A case-control study of 32,702 veterans," *Annals of Internal Medicine*, vol. 123, pp. 904–910, 1995.

[2] S. J. Winawer, A. G. Zauber, M. N. Ho et al., "Prevention of colorectal cancer by colonoscopic polypectomy," *The New England Journal of Medicine*, vol. 329, pp. 1977–1981, 1993.

[3] J. C. van Rijn, J. B. Reitsma, J. Stoker, P. M. Bossuyt, S. J. van Deventer, and E. Dekker, "Polyp miss rate determined by tandem colonoscopy: a systematic review," *The American Journal of Gastroenterology*, vol. 101, no. 2, pp. 343–350, 2006.

[4] N. J. Samadder, K. Curtin, T. M. Tuohy et al., "Characteristics of missed or interval colorectal cancer and patient survival: a population-based study," *Gastroenterology*, vol. 146, no. 4, pp. 950–960, 2014.

[5] T. Lee, C. Rees, R. Blanks et al., "Colonoscopic factors associated with adenoma detection in a national colorectal cancer screening program," *Endoscopy*, vol. 46, pp. 203–211, 2014.

[6] J. E. East, B. P. Saunders, D. Burling, D. Boone, S. Halligan, and S. A. Taylor, "Surface visualization at CT colonography simulated colonoscopy: effect of varying field of view and retrograde view," *The American Journal of Gastroenterology*, vol. 102, no. 11, pp. 2529–2535, 2007.

[7] V. Konda, S. S. Chauhan, B. K. Dayyeh et al., "Endoscopes and devices to improve colon polyp detection," *Gastrointestinal Endoscopy*, vol. 81, no. 5, pp. 1122–1129, 2015.

[8] N. K. Nikolova, *Introduction to Microwave Imaging*, Cambridge University Press, Cambridge, 2017.

[9] D. O'Loughlin, M. O'Halloran, B. M. Moloney, M. Glavin, E. Jones, and M. A. Elahi, "Microwave breast imaging: clinical advances and remaining challenges," *IEEE Transactions on Biomedical Engineering*, vol. 65, no. 11, pp. 2580–2590, 2018.

[10] M. Guardiola, S. Buitrago, G. Fernández-Esparrach et al., "Dielectric properties of colon polyps, cancer, and normal mucosa: ex vivo measurements from 0.5 to 20 GHz," *Medical Physics*, vol. 45, pp. 3768–3782, 2018.

[11] M. Guardiola, K. Djafri, M. Challal et al., "Design and evaluation of an antenna applicator for a microwave colonoscopy system," *IEEE Transactions on Antennas and Propagation*, vol. 67, no. 8, pp. 4968–4977, 2019.

[12] A. Garrido, R. Sont, W. Dghoughi et al., "Phantom validation of polyp automatic detection using microwave endoscopy for colorectal cancer prevention and early detection," 2021, http://www.researchsquare.Com/Article/Rs-479847/V1.

[13] P. McCulloch, J. A. Cook, D. G. Altman, C. Heneghan, M. K. Diener, and On behalf of the IDEAL group, "IDEAL framework for surgical innovation 1: the idea and development stages," *BMJ*, vol. 346, 2013.

[14] C. P. Pennell, A. D. Hirst, W. B. Campbell et al., "Practical guide to the idea, development and exploration stages of the IDEAL framework and recommendations," *The British Journal of Surgery*, vol. 103, pp. 607–615, 2016.

[15] A. Hirst, Y. Philippou, J. Blazeby et al., "No surgical innovation without Evaluation," *Annals of Surgery*, vol. 269, no. 2, pp. 211–220, 2019.

4. CV de la investigadora principal

CV Date	29/09/2022

Part A. PERSONAL INFORMATION

First Name	Marta		
Family Name	Guardiola Garcia		
Sex	Female	Date of Birth	10/10/1984
ID number Social Security, Passport	77915094H		
URL Web			
Email Address	marta@miwendo.com		
Open Researcher and Contributor ID (ORCID)	0000-0002-8751-5378		

A.1. Current position

Job Title	CTO, Co-Founder & President		
Starting date	2020		
Institution	MiWEndo Solutions S.L.		
Department / Centre			
Country		Phone Number	
Keywords			

A.2. Previous positions (Research Career breaks included)

Period	Job Title / Name of Employer / Country
2021 - 2022	Profesora Asociada / Universitat Internacional de Catalunya
2014 - 2021	Profesora asociada / Universidad Pompeu Fabra
2014 - 2019	Investigador postdoctoral / Universidad Pompeu Fabra
2009 - 2013	Estudiante de doctorado / Universitat Politècnica de Catalunya
2006 - 2009	Becario de asistencia a la investigación / Universitat Politècnica de Catalunya

A.3. Education

Degree/Master/PhD	University / Country	Year
Doctor en Programa Oficial de Teoria del senyal i comunicacions	Universitat Politècnica de Catalunya	2013
Master of Science in Research on Information and Communication Technologies	Universitat Politècnica de Catalunya	2009
Ingeniero Telecomunicación	Universitat Politècnica de Catalunya	2008

Part B. CV SUMMARY

Marta Guardiola received the M.Sc. degree in telecommunications and the Ph.D. from the Universitat Politècnica de Catalunya, Spain, in 2009 and 2013 respectively. In 2012 she was at University of Bristol for a research stay. From 2014 to 2019, she was a Post-Doctoral researcher with the Department of Information and Communications Technologies, Universitat Pompeu Fabra, Spain. Her research interest is microwave imaging for medical applications, including imaging algorithms, computational models, electromangetic simulations, design and manufacturing of microwave imaging acquisition systems and preclinical studies. In 2019, she co-founded MiWEndo Solutions, a Spinoff of several Catalan research institutions devoted to the development of a microwave colonoscopy system. In MiWEndo solutions she serves as the President of the Board of Directors and Chief Technology Officer. She has authored dozens of publications in peer-reviewed journals and conferences, holds a patent and has received several grants including the EIC Accelerator from the European Commission. As a result of her work, she has received more than 10 awards including the recognition of the Scientific

Journal Nature in its Spinoff Prize. She received training in entrepreneurship from University of California Berkeley and EOI Business School. She is Associate Professor in Universitat Internacional de Catalunya and Universitat Pompeu Fabra.

Part C. RELEVANT ACCOMPLISHMENTS

C.1. Most important publications in national or international peer-reviewed journals, books and conferences

AC: corresponding author. (nº x / nº y): position / total authors. If applicable, indicate the number of citations

1 **Scientific paper**. Marta Guardola; Walid Dhgoughi; Roberto Sont; Alejandra Garrido; Sergi Marcoval; Luz María Neira; Ignasi Belda; Glòria Fernandez. 2022. MiWEndo: Evaluation of aMicrowave Colonoscopy Algorithmfor Early Colorectal Cancer Detection in Ex Vivo Human ColonModels Sensors. 22-4902.

2 **Scientific paper**. Gloria Fernandez; Alejandra Garrido; Roberto Sont; et al;. 2022. Microwave-based colonoscopy. preclinical evaluation in an ex vivo human colon model Gastroenterology Research and Practice. Hindawi Limited. 2022-9522737.

3 **Scientific paper**. Alejandra Garrido; Roberto Sont; Walid Dghoughi; Sergi Marcoval; Jordi Romeu; Glòria Fernandez; Ignasi Belda; Marta Guardiola. 2021. Automatic Polyp Detection Using Microwave Endoscopy for Colorectal Cancer Prevention and Early Detection: Phantom Validation IEEE Access. IEEE.

4 **Scientific paper**. Guardiola, M.; Djafri, K.; Challal, M.; Ballester, M. A. G.; Fernandez-Esparrach, G.; Camara, O.; Romeu}, J.2019. Design and Evaluation of an Antenna Applicator for a Microwave Colonoscopy System IEEE Transactions on Antennas and Propagation. pp.1-1. ISSN 0018-926X.

5 **Scientific paper**. 2018. Dielectric properties of colon polyps, cancer, and normal mucosa: Ex vivo measurements from 0.5 to 20 GHz Medical Physics. 45-8.

6 **Scientific paper**. Guardiola, M.; Capdevila, S.; Romeu, J.; Jofre, L.2012. 3-D microwave magnitude combined tomography for breast cancer detection using realistic breast models IEEE Antennas and Wireless Propagation Letters. 11, pp.1548-1551. ISSN 15361225.

7 **Scientific paper**. Guardiola, M.; Monsalve, B.; Calafell, I.; Roqueta, G.; Romeu, J.2012. Fabrication and measurement of homemade standard antennas IEEE Antennas and Propagation Magazine. 54-1, pp.177-194. ISSN 10459243.

8 **Scientific paper**. Guardiola, M.; Jofre, L.; Capdevila, S.; Blanch, S.; Romeu, J.2011. 3D UWB Magnitude-Combined tomographic imaging for biomedical applications. Algorithm validation Radioengineering. 20-2, pp.366-372. ISSN 12102512.

9 **Popular science article**. Walid Dghoughi; Alejandra Garrido; Ignasi Belda; Glòria Fernandez; Marta Guardiola; Roberto Sont; Sergi Marcoval; Walid Dghoughi. 2021. Alternativas a la colonoscopia para detectar el cáncer a tiempo The conversation. ASOCIACION THE CONVERSATION ESPAÑA.

C.2. Conferences and meetings

1 MiWEndo: Microwave Endoscopy System for Early Detection of Colorectal Cancer. Challenges in the Industrialization and Preclinical Phase. European Conference on Antennas and Propagation. European Association on Antennas and Propagation. 2022. Spain.

2 Preliminary phantom-based dynamic calibration techniques assessment for microwave colonoscopy systems. European Conference on Antennas and Propagation. European Association on Antennas and Propagation. 2022. Spain.

3 MiWEndo Solutions. Mujeres investigadoras innovan. Universidad de Granada. 2021. Spain.

4 Judit Chamorro; Marta Guardiola; Miguel Angel Gonzalez Ballester; Roberto Sont; Lluis Jofre; Gloria Fernandez; Oscar Camara. Sensitivity analysis of a new imaging device for endoscopic explorations. International Conference on Industrial and Applied Mathematics. ICIAM. 2019. Spain.

5 Marta Guardiola; Jordi Romeu; Gloria Fernandez-Esparrach; Miguel Angel Gonzalez-Ballester; Oscar Camara. In silico and ex vivo validation of a microwave endoscopic system for colon examinations. Computer Assisted Radiology and Surgery (CARS). CARS. 2017. Germany.
6 Marta Guardiola; Mario Ceresa; Jordi Romeu; Gloria Fernandez-Esparrach; Miguel Angel Gonzalez-Ballester; Oscar Camara. Microwave endoscopy for colorectal cancer prevention. Computer Assisted Radiology and Surgery (CARS). CARS. 2017. Spain.
7 Marta Guardiola; Santiago Buitrago; C Chen; Jordi Romeu; Lluis Jofre. Microwave Breast Imaging Using a Non-Conventional Magnitude-Combined Approach. International Microwave Workshop Series on RF and Wireless Technologies for Biomedical and Healthcare Applications (IMWS-Bio 2015). IEEE MTT-S. 2015. Taiwan.
8 Marta Guardiola; Ali Pashaei; Rafael Sebastian; Alejandro Lopez; Juan Acosta; David Andreu; Antonio Berruezo; Oscar Camara. Computational electrophysiology for prediction of the outflow tract origin in idiopathic ventricular tachycardia. 2015 Cardiac Physiome Workshop. Cardiac Physiome Society. 2015. New Zealand.
9 Marta Guardiola; Santiago Buitrago; Lluis Jofre. Towards microwave system for real-time medical imaging. 2014 IEEE Conference on Antenna Measurements Applications (CAMA). IEEE Antennas and Propagation Society. 2014. France.
10 Marta Guardiola; Santiago Capdevila; Lluis Jofre. Robust differential multi-frequency microwave imaging for breast cancer detection. 7th European Conference on Antennas and Propagation (EuCAP 2013). European Association on Antennas and Propagation. 2013. Sweden.
11 Gemma Roqueta; Marta Guardiola; Santiago Capdevila; Lluís Jofre Roca. Robust differential multifrequency microwave biomedical imaging. 32nd Progress in Electromagnetics Research Symposium (PIERS),. Progress in Electromagnetics Research. 2012. Russia.
12 M. Guardiola; L. Jofre; J. Romeu. UWB magnitude combined realistic breast model imaging capabilities. Antennas and Propagation Society International Symposium (APSURSI), 2012. IEEE. 2012. United States of America.
13 M. Guardiola; L. Jofre; S. Capdevila; J. Romeu. UWB brain differential imaging capabilities. Antennas and Propagation (EUCAP), 2012 6th European Conference on. European Association on Antennas and Propagation (EurAAP). 2012. Czech Republic.
14 S. Capdevila; G. Roqueta; M. Guardiola; L. Jofre; J. Romeu; J. Bolomey. Water infiltration detection in civil engineering structures using RFID. Antennas and Propagation (EUCAP), 2012 6th European Conference on. European Association on Antennas and Propagation (EurAAP). 2012. Czech Republic.
15 Lluís Jofre; Jordi Romeu; Santiago Capdevila; Gemma Roqueta; Marta Guardiola. Semi-embedded RFID sensor networks for imaging application. Conference on Electromagnetic Near-Veld Characterization and Imaging (ICONIC), 2011.. IEEE. 2011. France.
16 M. Guardiola; A. Fhager; L. Jofre; M. Persson. Circular microwave tomographic imaging. experimental comparison between quantitative and qualitative algorithms. Antennas and Propagation (EUCAP). European Association on Antennas and Propagation. 2011. Italy.
17 M. Guardiola; L. Jofre; F. Gedda; S. Capdevila; J. Romeu; S. Blanch. 3D arrayed microwave tomographic system for medical imaging. Wireless Information Technology and Systems (ICWITS), 2010 IEEE International Conference on. IEEE. 2010. United States of America.
18 M. Guardiola; L. Jofre; J. Romeu. 3D UWB tomography for medical imaging applications. Antennas and Propagation Society International Symposium (APSURSI), 2010 IEEE. Institute of Electrical and Electronics Engineers (IEEE). 2010. Canada.
19 E. Nova; J. Abril; M. Guardiola; S. Capdevila; A. Broquetas; J. Romeu; L. Jofre. Terahertz subsurface imaging system. Antennas and Propagation (EuCAP), 2010. European Association on Antennas and Propagation (EurAAP). 2010. Spain.
20 M. Guardiola; L. Jofre; S. Capdevila; S. Blanch; J. Romeu. Toward 3D UWB tomographic imaging system for breast tumor detection. Antennas and Propagation (EuCAP), 2010. European Association on Antennas and Propagation (EurAAP). 2010. Spain.

21 M. Guardiola; S. Capdevila; S. Blanch; J. Romeu; L. Jofre. UWB high-contrast robust tomographic imaging for medical applications. Electromagnetics in Advanced Applications, 2009. ICEAA '09. International Conference on. IEEE. 2009. Italy.

22 M. Guardiola; S. Capdevila; L. Jofre. UWB BiFocusing Tomography for Breast Tumor Detection. Antennas and Propagation, 2009. EuCAP 2009. 3rd European Conference on. European Association on Antennas and Propagation (EurAAP). 2009. Germany.

23 Terahertz tomographic imaging technologies. XXIV Simposium Nacional de la Unión Científca Internacional de Radio (URSI), 2009. URSI. 2009. Spain.

24 S. Capdevila; M. Jofre; J. Rodriguez; M. Guardiola; A. Papio; F. De Flaviis; L. Jofre. UWB MST MEMS-based near-field imaging system. Antennas and Propagation Society International Symposium, 2008. IEEE. 2008. United States of America.

C.3. Research projects and contracts

1 **Project**. Revolutionary electromagnetic endoscopy accessory to automatize polyp detection; MiWEndo. Comisión Europea. (MiWEndo Solutions). 01/10/2020-30/09/2023. 2.800.000 €.

2 **Project**. Medidas legales y fiscales para el mantenimiento de las empresas. Ministerio de Ciencia e Innovación. 2020-2023. 25.410 €.

3 **Project**. Industrialization and preclinical validation of a medical device for microwave-assisted endoscopy. European Insitute of Innovation and Technology. (MiWEndo Solutions). 15/07/2020-14/07/2021. 50.000 €.

4 **Project**. Desarrollo Tecnológico en Salud. (Institut d`Investigacions Biomèdiques August Pi i Sunyer). 2018-2020. 75.000 €.

5 **Project**. Optimization and validation of a microwave imaging protoype for endoscopic explorations and interventions (MiWEndo). AGENCIA DE GESTIO D'AJUTS UNIVERSITARIS I DE RECERCA. Oscar Camara Rey. (Universidad Pompeu Fabra). 25/07/2017-25/01/2019. 99.990 €.

6 **Project**. Real-Time Microwave Imaging Device for Endoscopic Explorations and Interventions. Obra Social Fundación la Caixa. (Universidad Pompeu Fabra). 2016-2018. 70.000 €.

7 **Project**. Real-Time Microwave Imaging Device for Endoscopic Explorations and Interventions (MiWEndo). Generalitat de Catalunya. Oscar Camara Rey. (Universidad Pompeu Fabra). 2015-2016. 25.000 €.

8 **Project**. Simulaciones rápidas de la electrofisiología del corazón basadas en señales e imágenes para la planificación asistida por ordenador de intervenciones clínicas (SAFE-PLAI). Ministerio de Ciencia e Innovación. Investigación. Oscar Camara Rey. (Universidad Pompeu Fabra). 2012-2014. 148.300 €.

9 **Project**. Terahertz Technology for Electromagnetic Sensing Applications (CSD-2008-00068). Ministerio de Ciencia e Innovación. (Universitat Politècnica de Catalunya). 2008-2013. 3.500.000 €.

10 **Project**. Design, simulation and measurement of millimeter wave antennas for communications and imaging (TEC2010-20841-C04-02). Comisión Interministerial de Ciencia y Tecnología. (Universitat Politècnica de Catalunya). 2010-2012. 215.000 €.

11 **Project**. Sistemas multiantenas reconfigurables para comunicaciones y sensores (TEC2007-66698-C04-01). Comisión Interministerial de Ciencia y Tecnología. (Universitat Politècnica de Catalunya). 2007-2009. 266.382 €.

12 **Contract**. Advanced materials for antenna development for automotive and spatial applications Ficosa International, S.A.. 2008-01/01/2010. 100.000 €.

C.4. Activities of technology / knowledge transfer and results exploitation

Marta Guardiola Garcia; Miguel Angel Gonzalez Ballester; Oscar Camara Rey; Mario Ceresa; Jordi Romeu Robert; Gloria Fernandez Esparrach. 40614008. A medical system and a device based on microwave technology for prevention and diagnosis of diseases Spain. 20/01/2016. Universidad Pompeu Fabra.